Figure 1
Schematics of the Types of IOM-CMS Materials

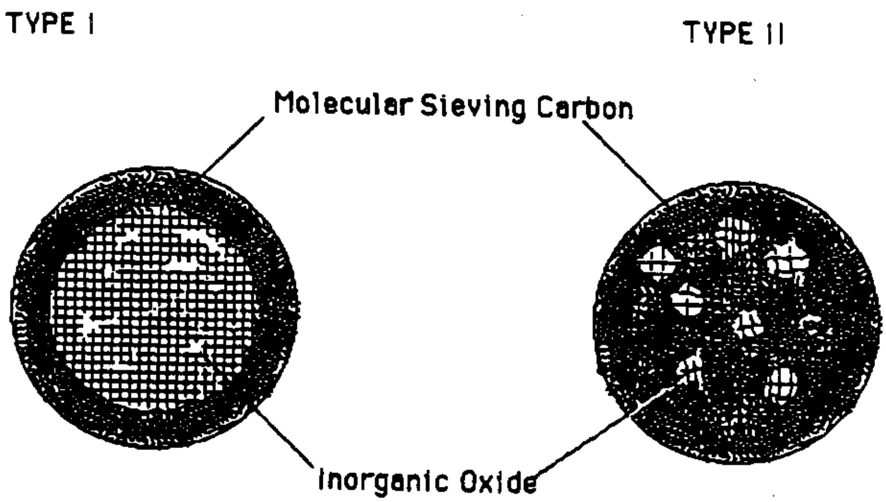

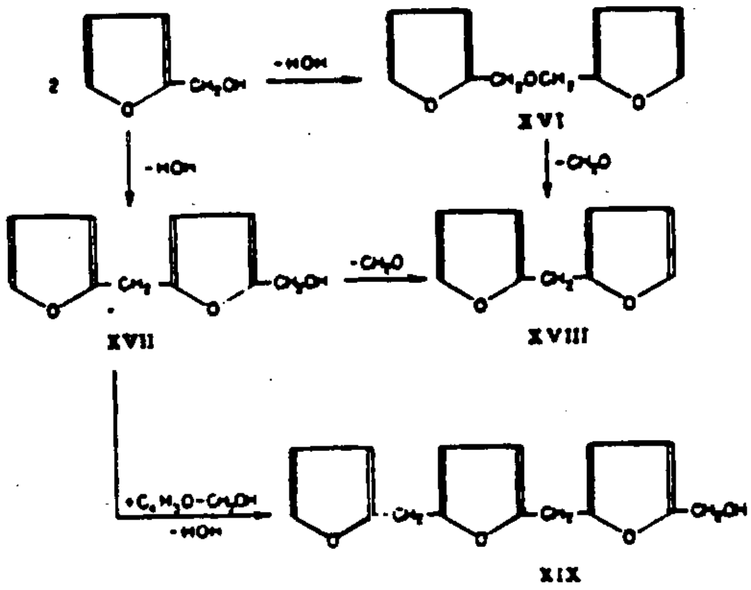

Figure 2

Pyrolytic Chemistry of PFA

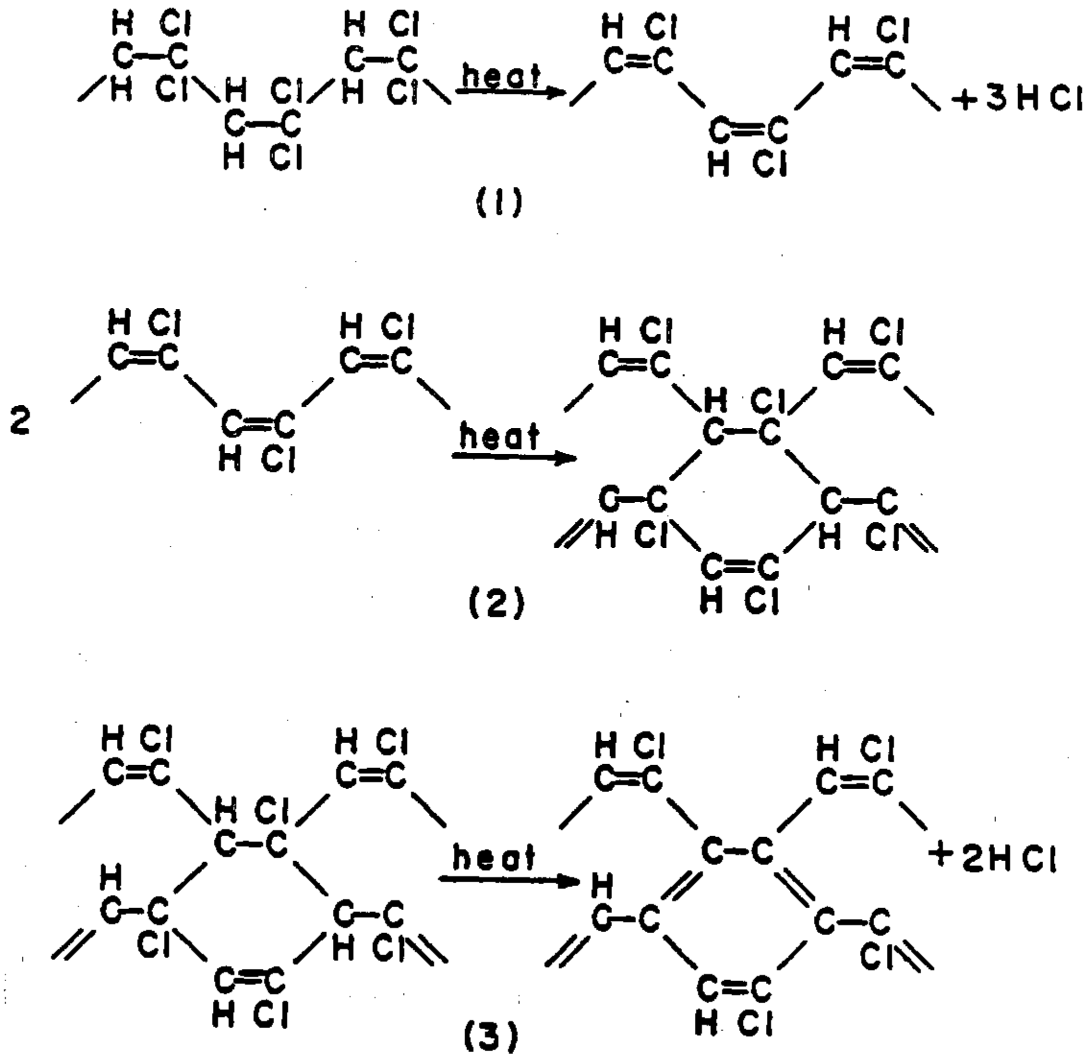

Figure 3

Pyrolytic Chemistry of PVC/PVDC

GRAVIMETRIC GAS ADSORPTION WITH SAMPLE CAROUSEL

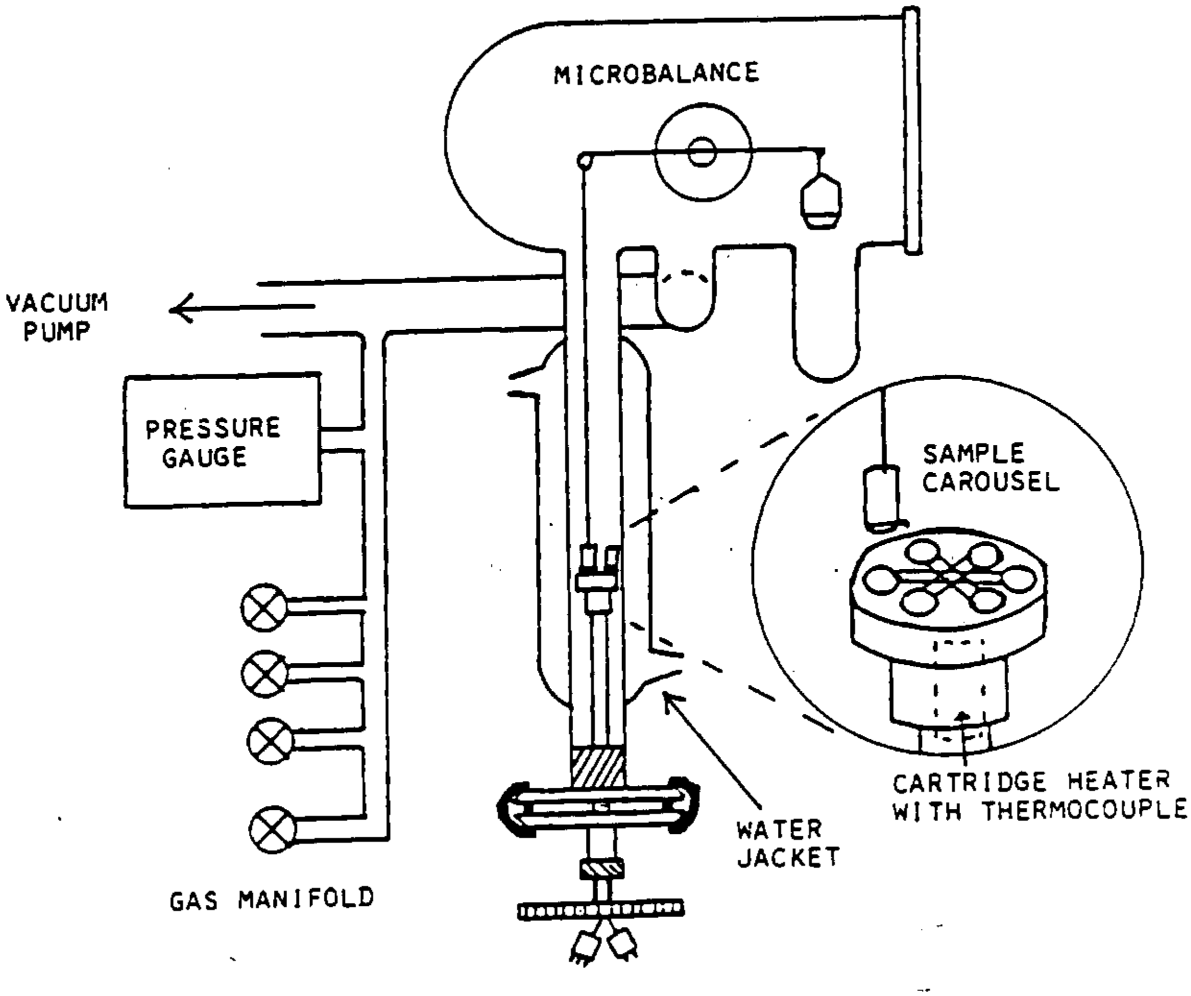

Figure 4

Molecular Probe Analysis Apparatus

N2 BET SURFACE AREA vs CO2 AREA
FIGURE 5.

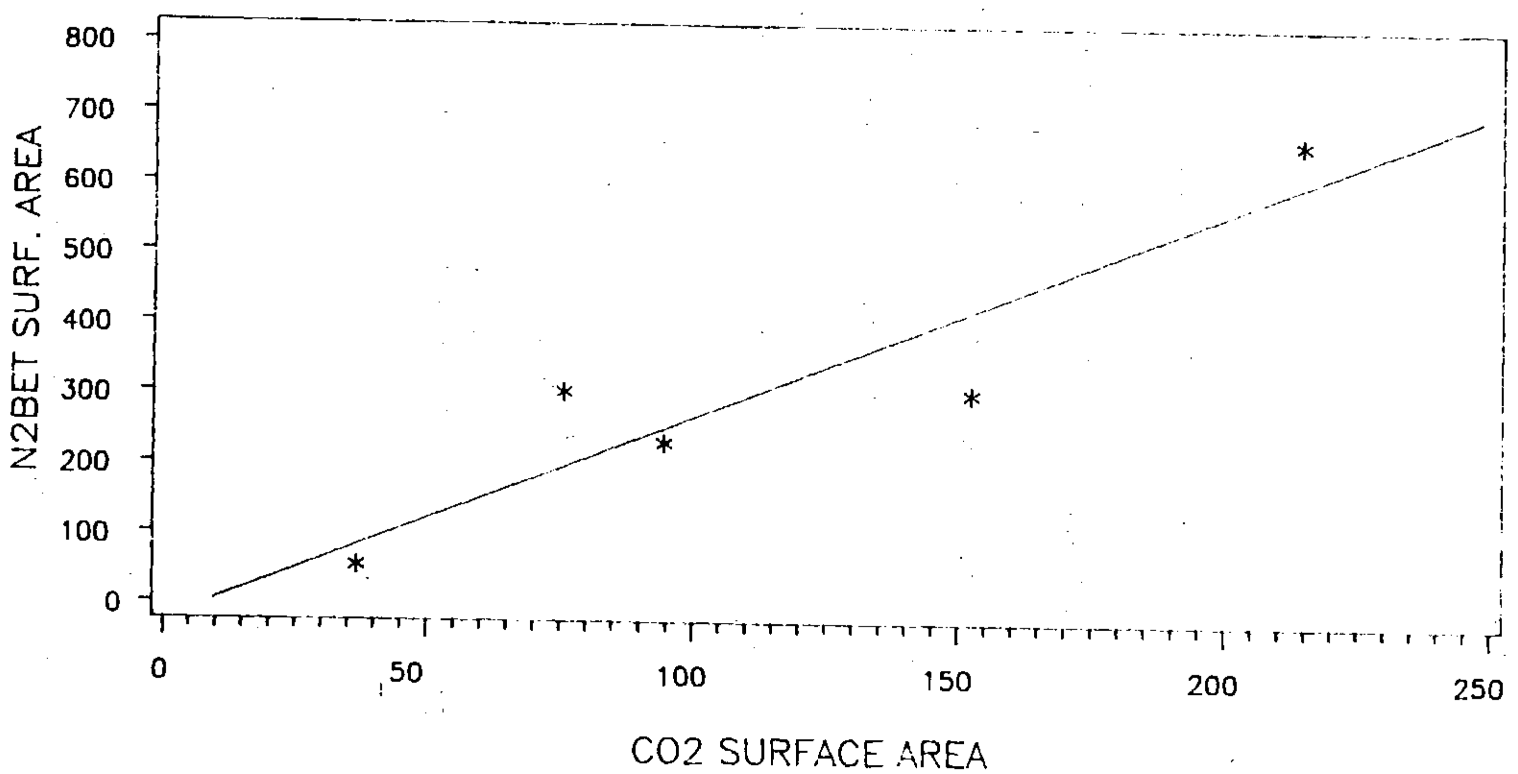

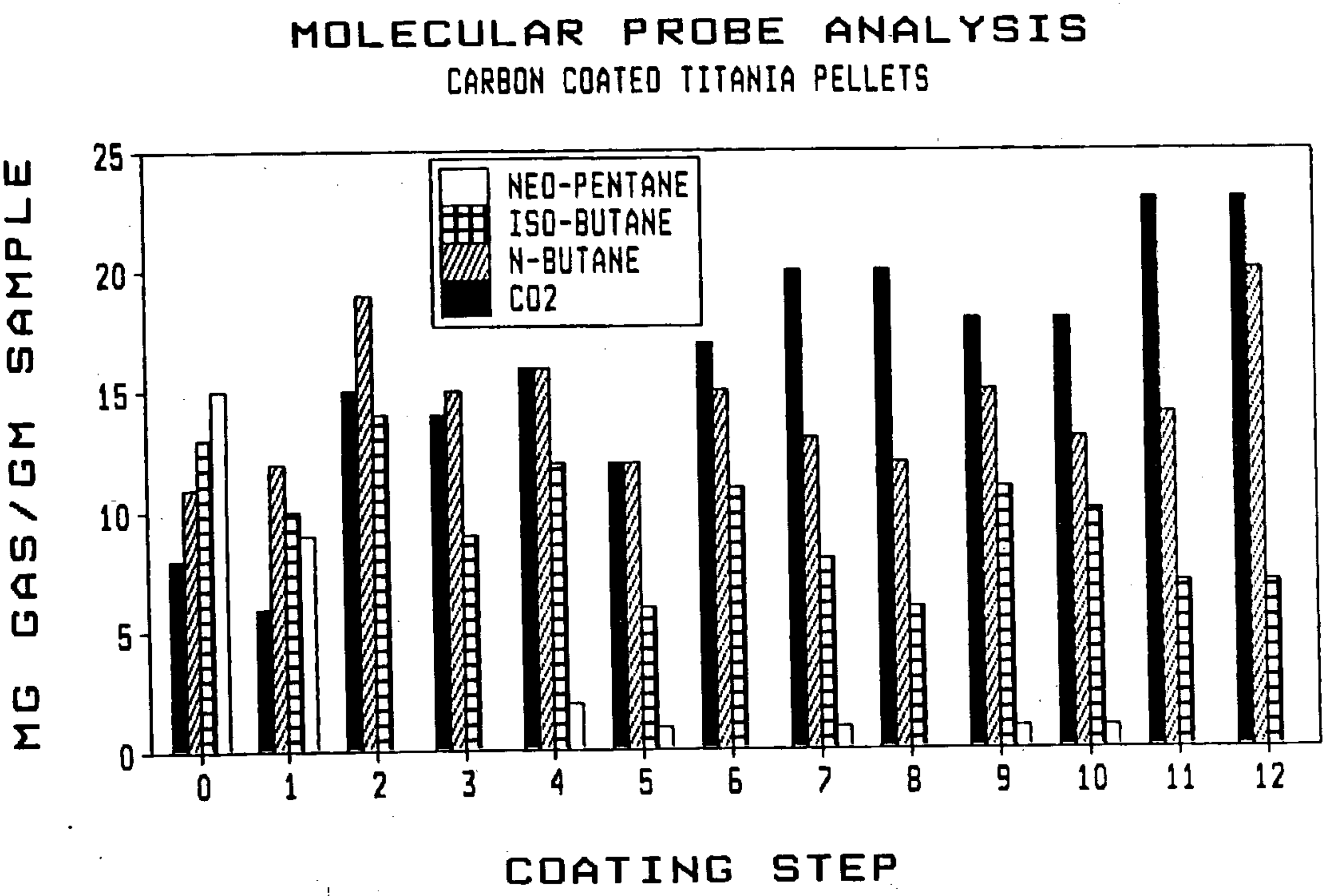

Figure 6

Molecular Probe Analyses for C-TiO_2 versus Coating Step

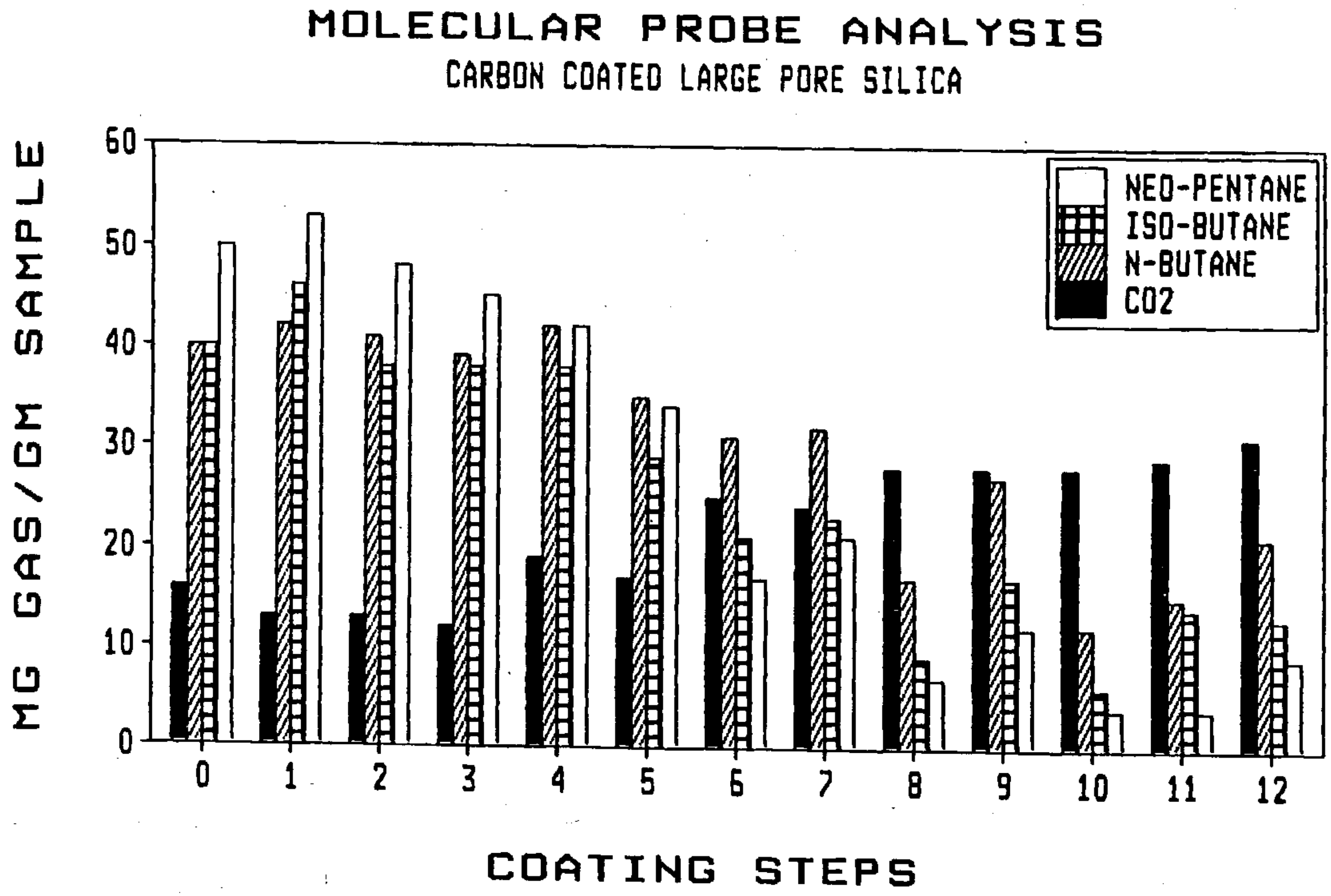

Figure 7

Molecular Probe Analyses for $C-SiO_2$ versus Coating Step

Figure 8

(a-f) Nitrogen Isotherms for $C-TiO_2$ versus Coating Step

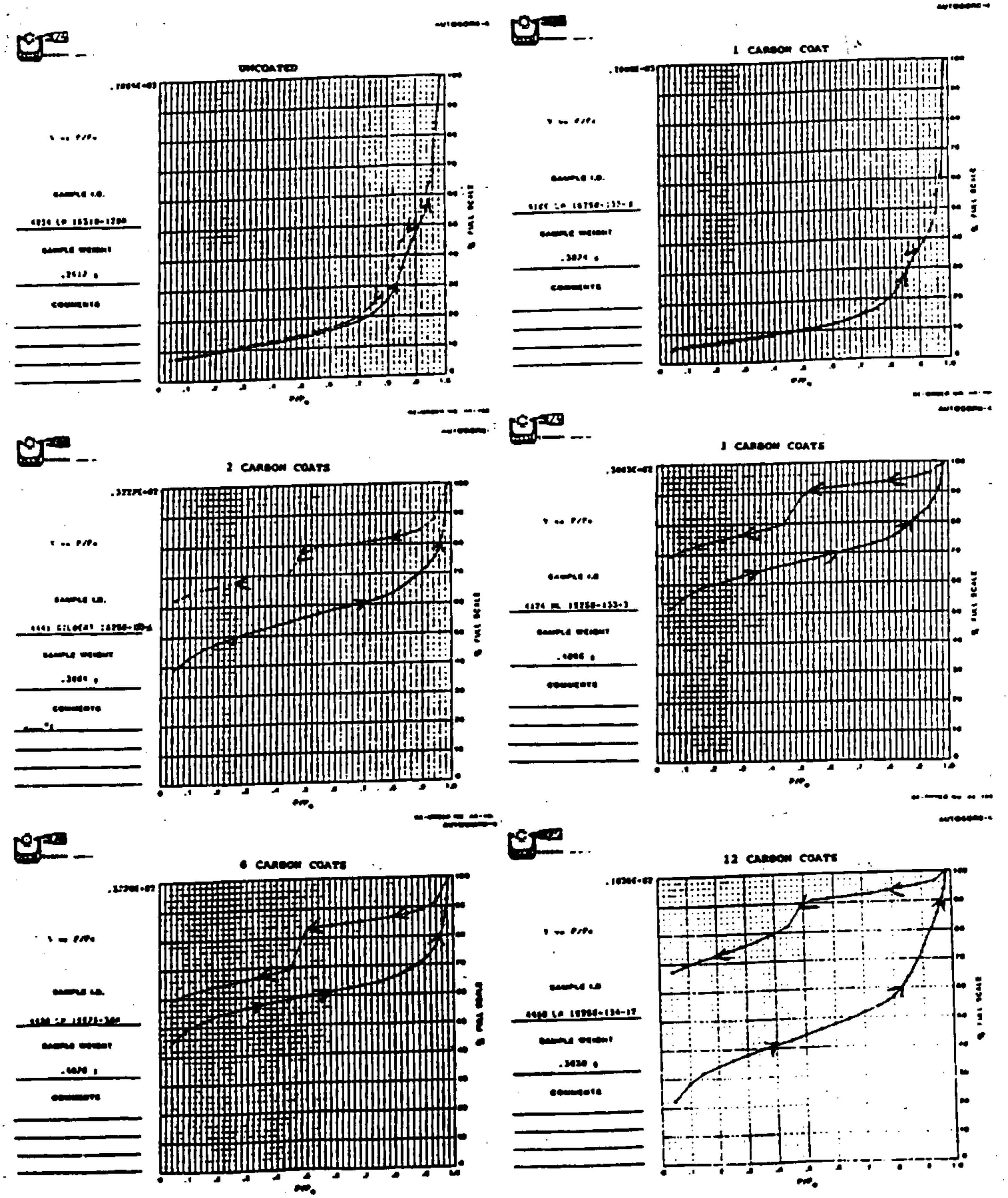

Figure 9

(a–e) Nitrogen Isotherms for C-SiO_2 versus Coating Step

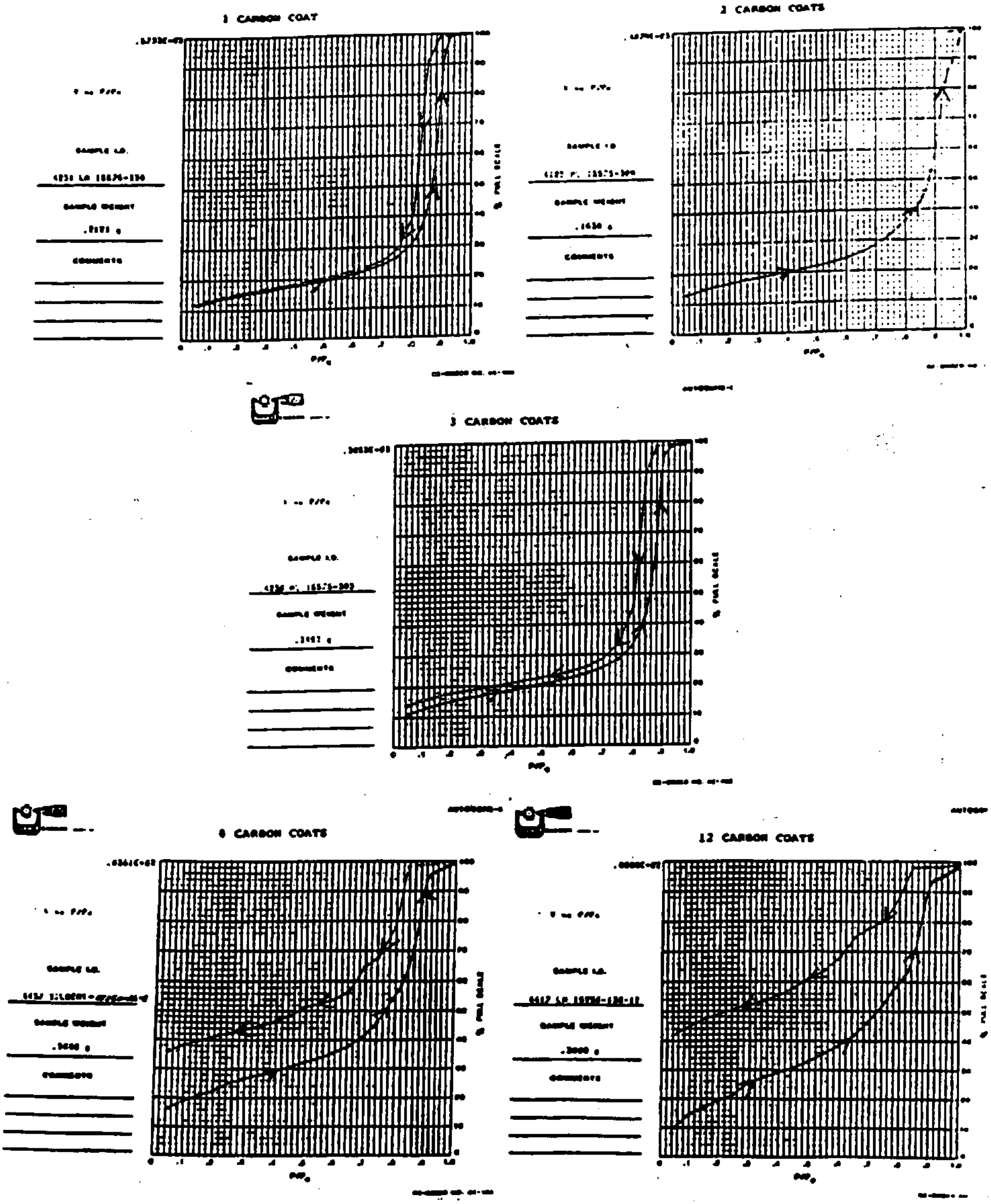

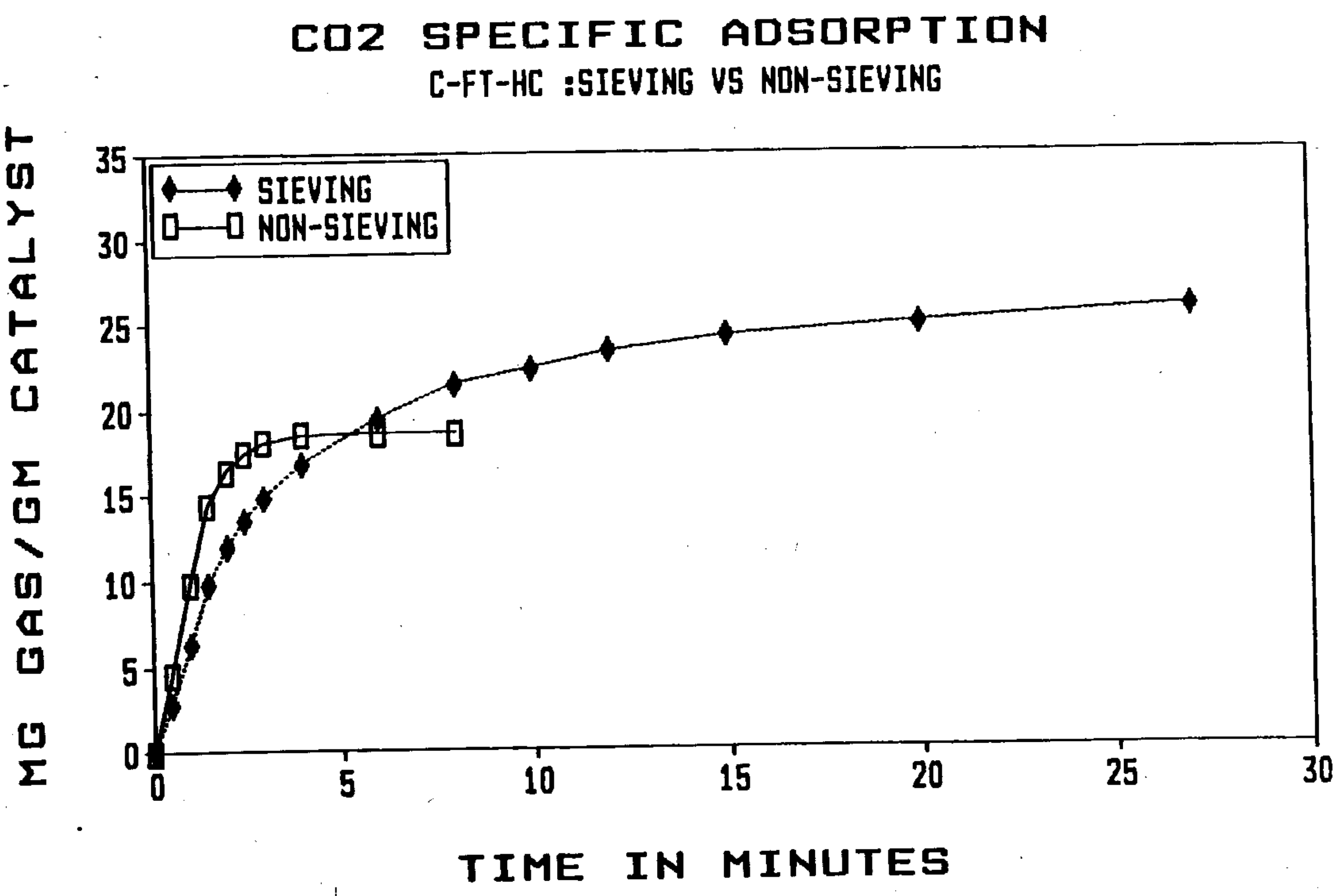

Figure 10

Adsorption of CO_2 on Type-I,C-FT-HC(1:1) versus Uncoated

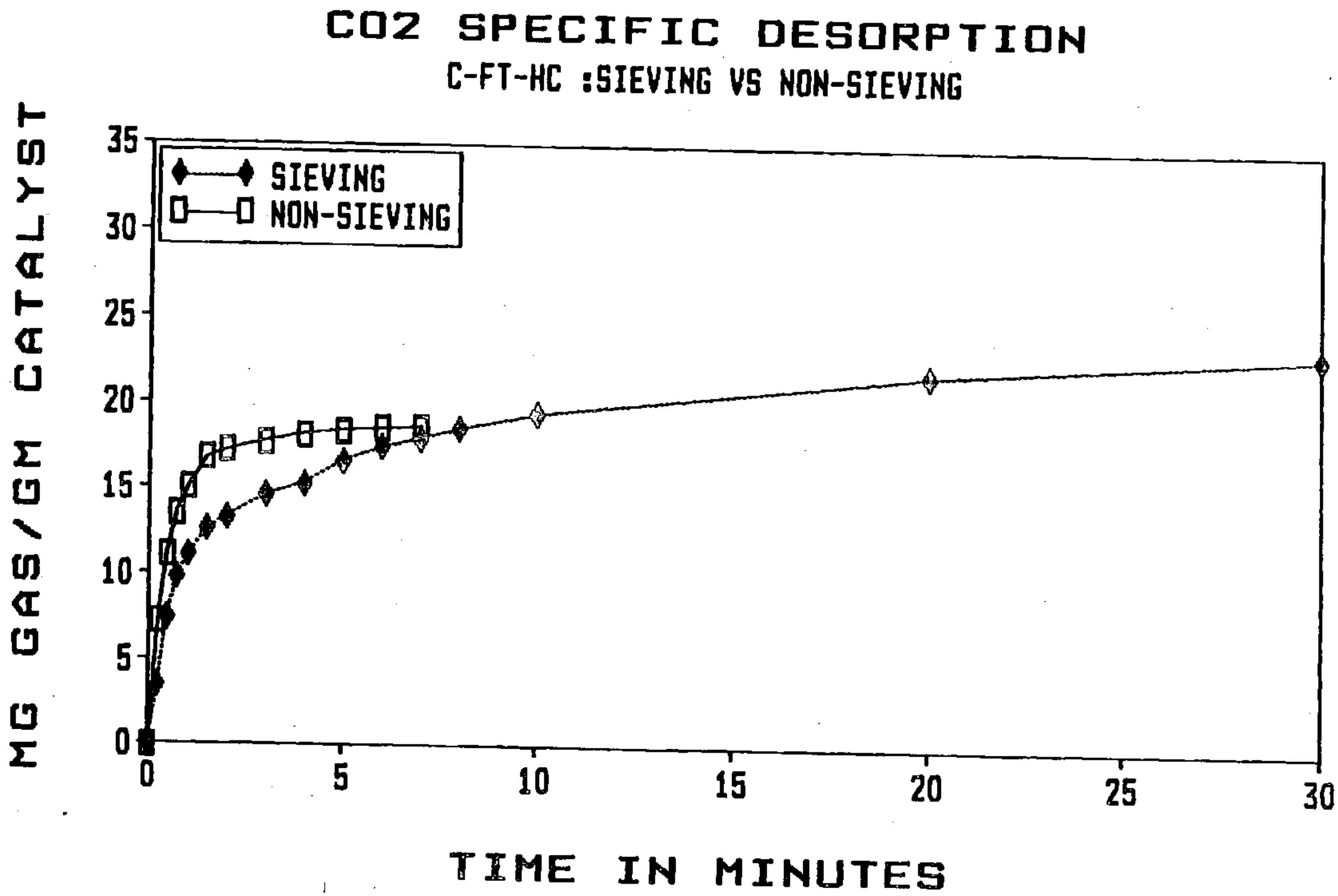

Figure 11

Desorption of CO_2 on Type-I,C-FT-HC(1:1) versus Uncoated

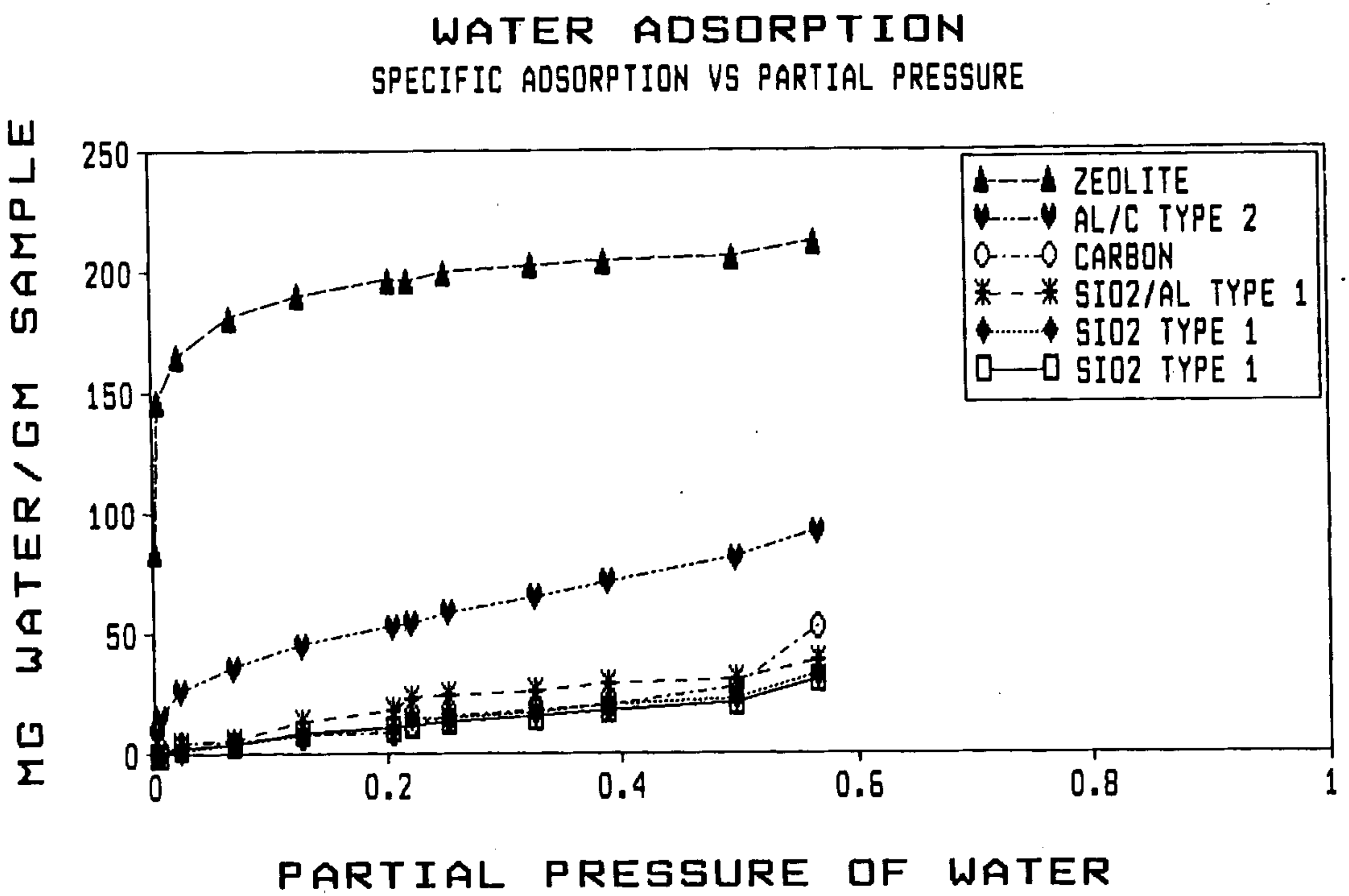

Figure 12

Water Adsorption Isotherms for IOM-CMS Materials

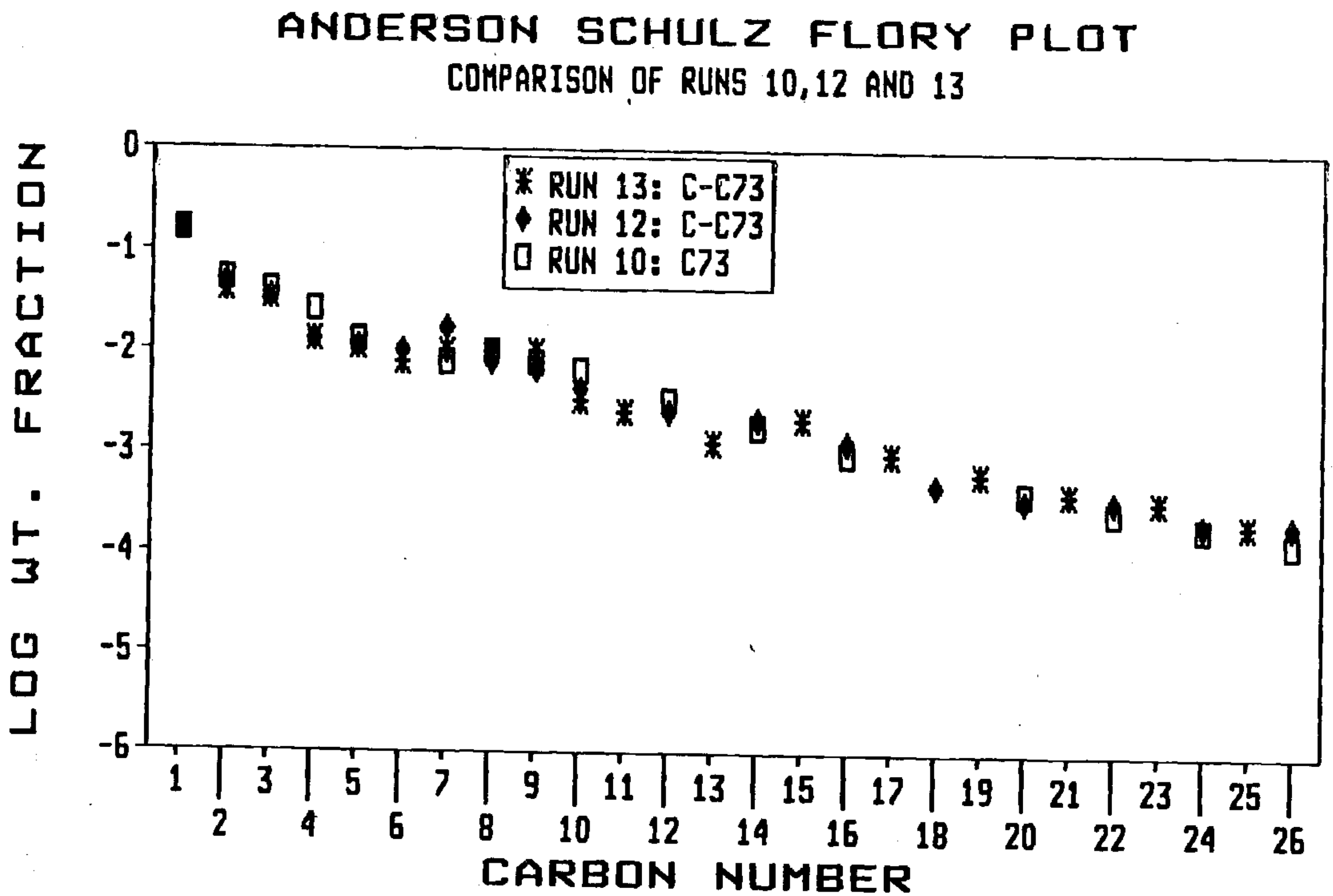

Figure 13 (a)

ASF Plots for Carbonized C-73 and Control

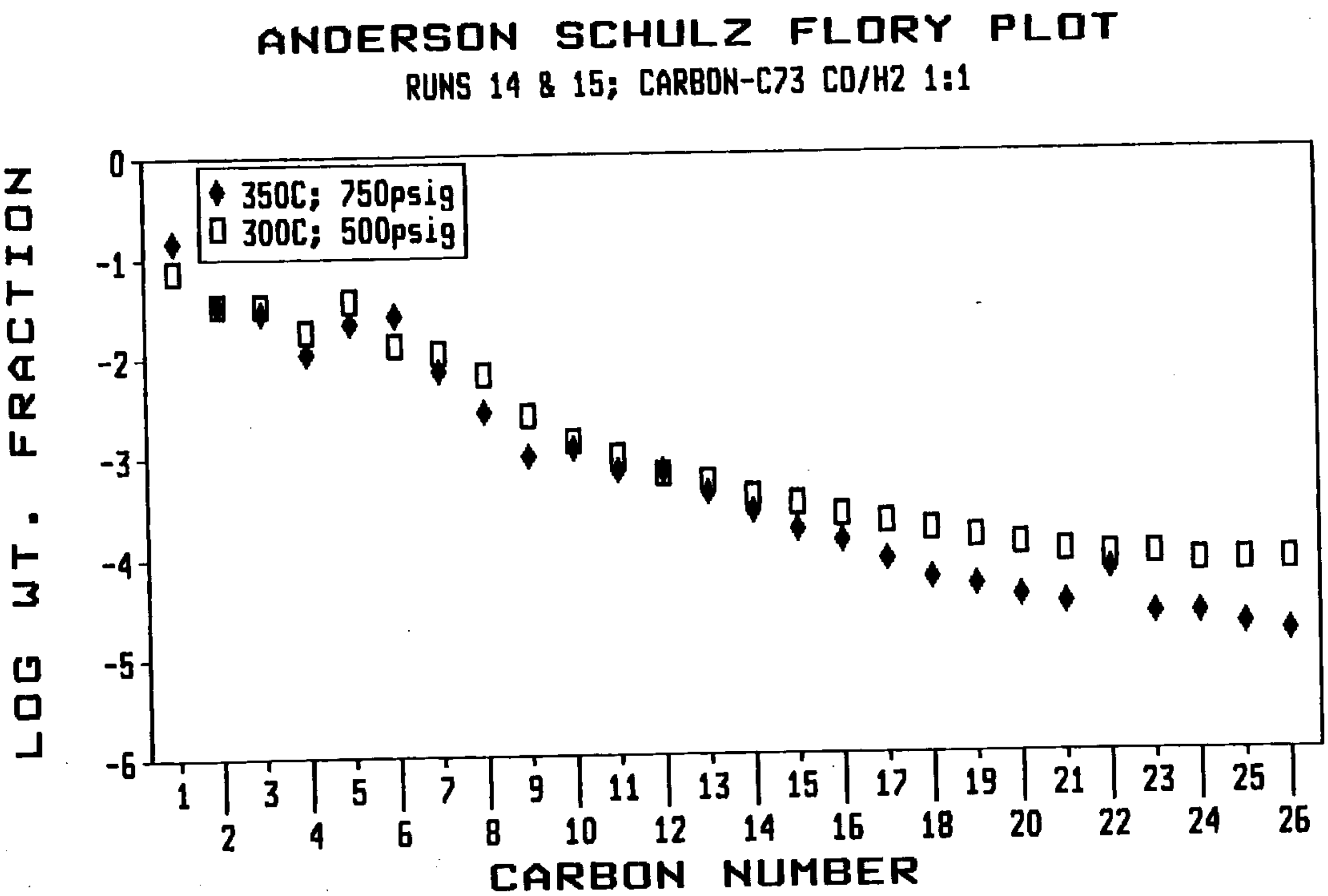

Figure 13 (b)

ASF Plots for Carbonized C-73 and Control

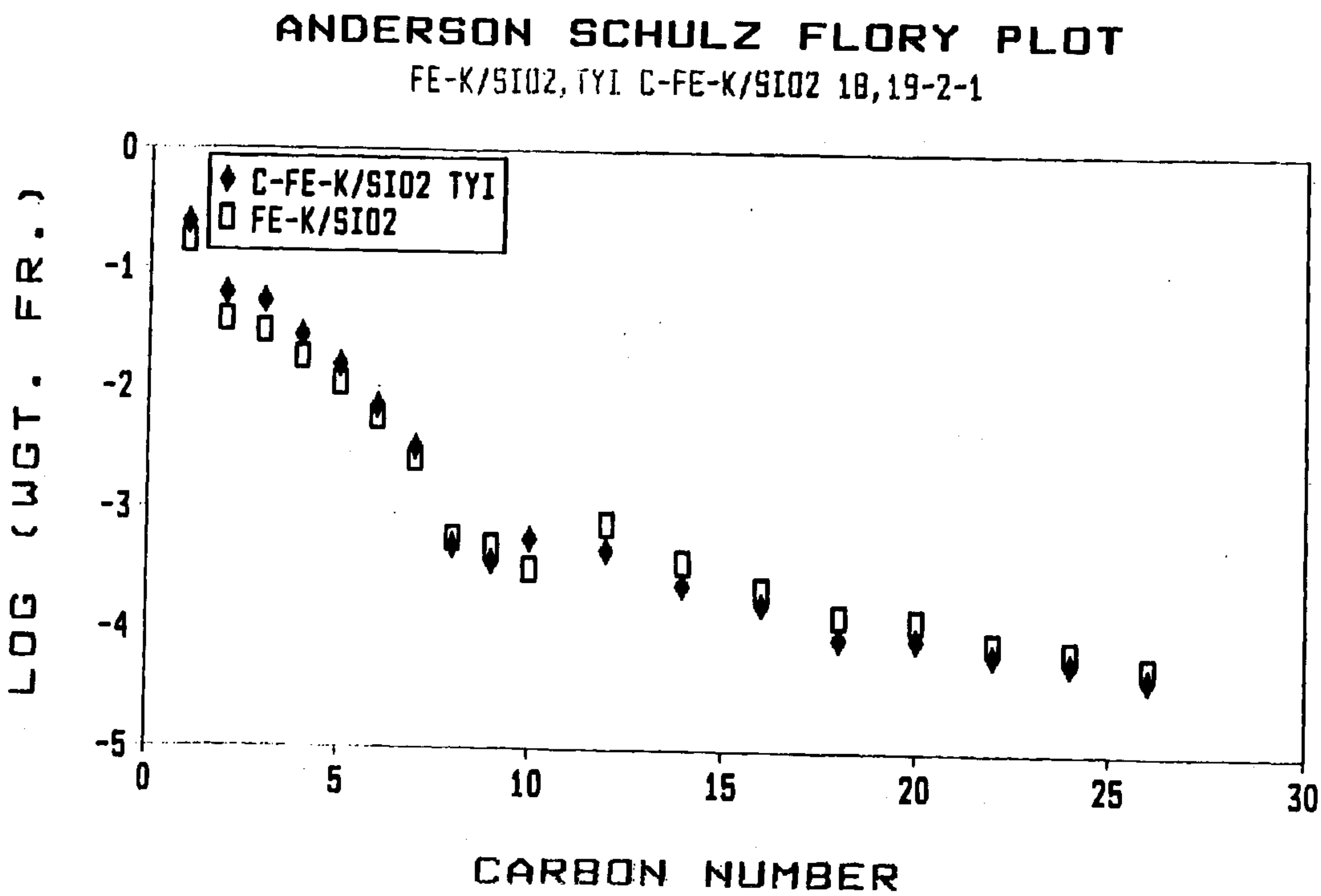

Figure 14(a)

ASF Plots for Carbonized Fe-K/SiO_2

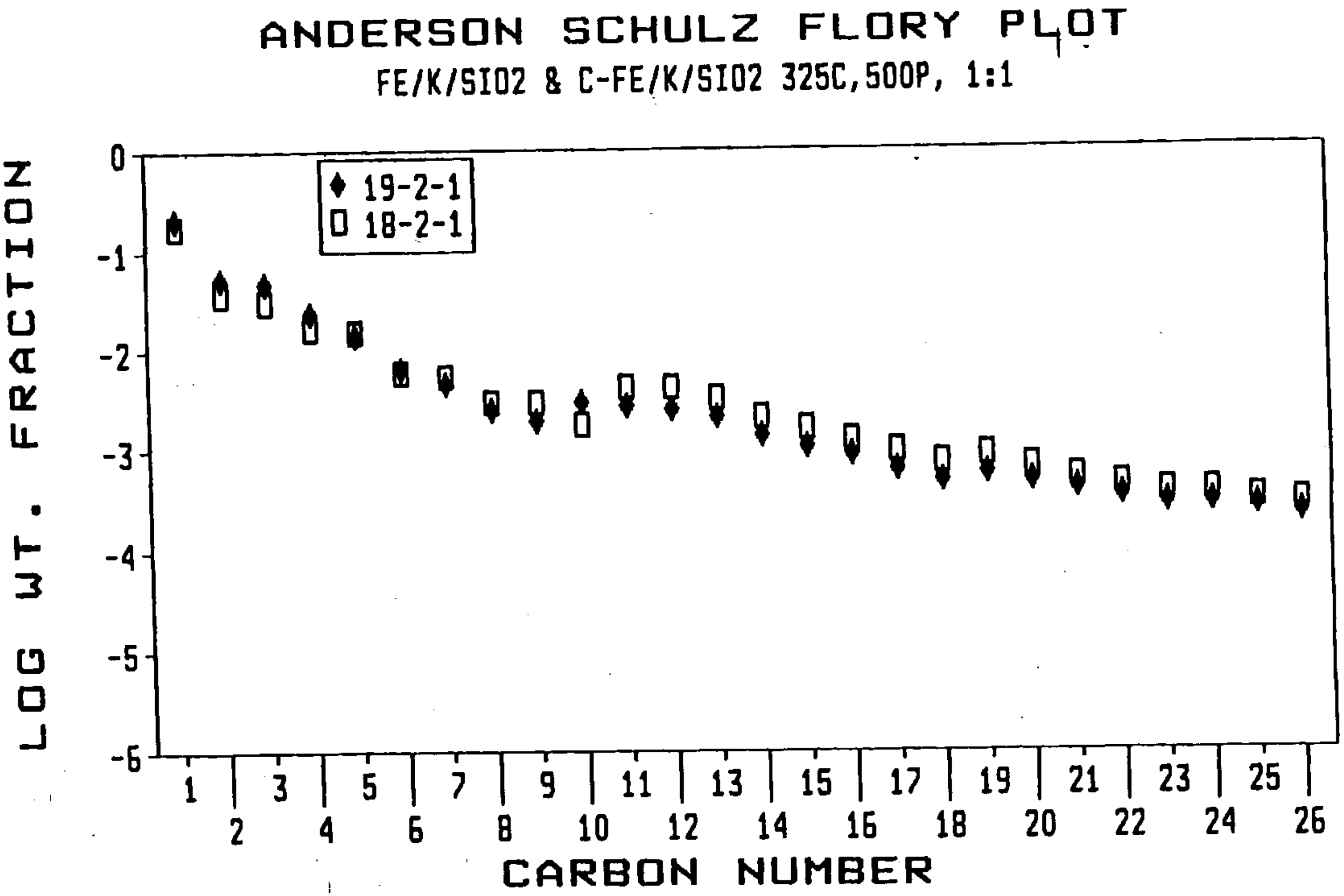

Figure 14 (b)

ASF Plots for Carbonized Fe-K/SiO_2

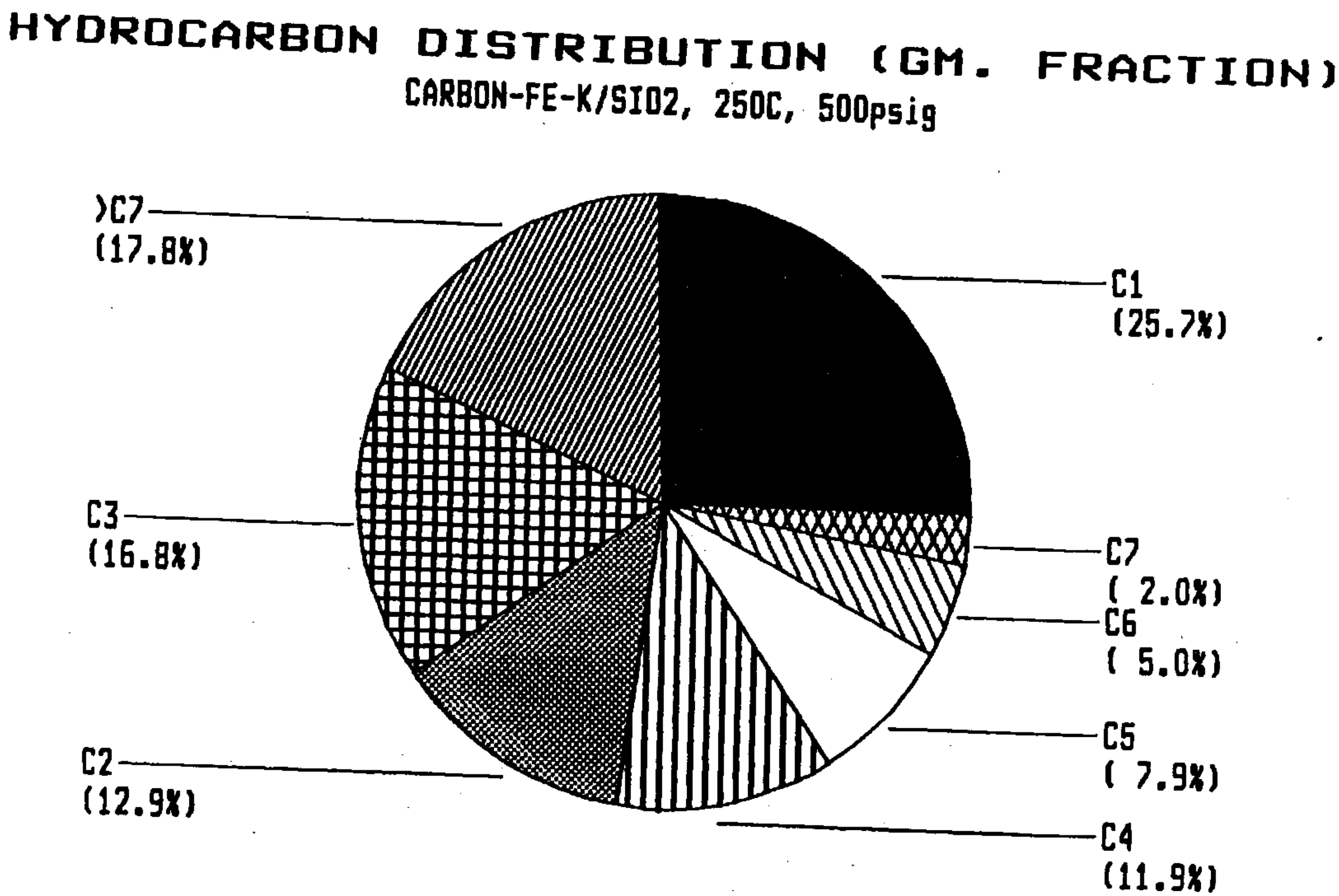

Figure 15 (a)

Gram Fractions of Products for Carbonized Fe-K/SiO_2

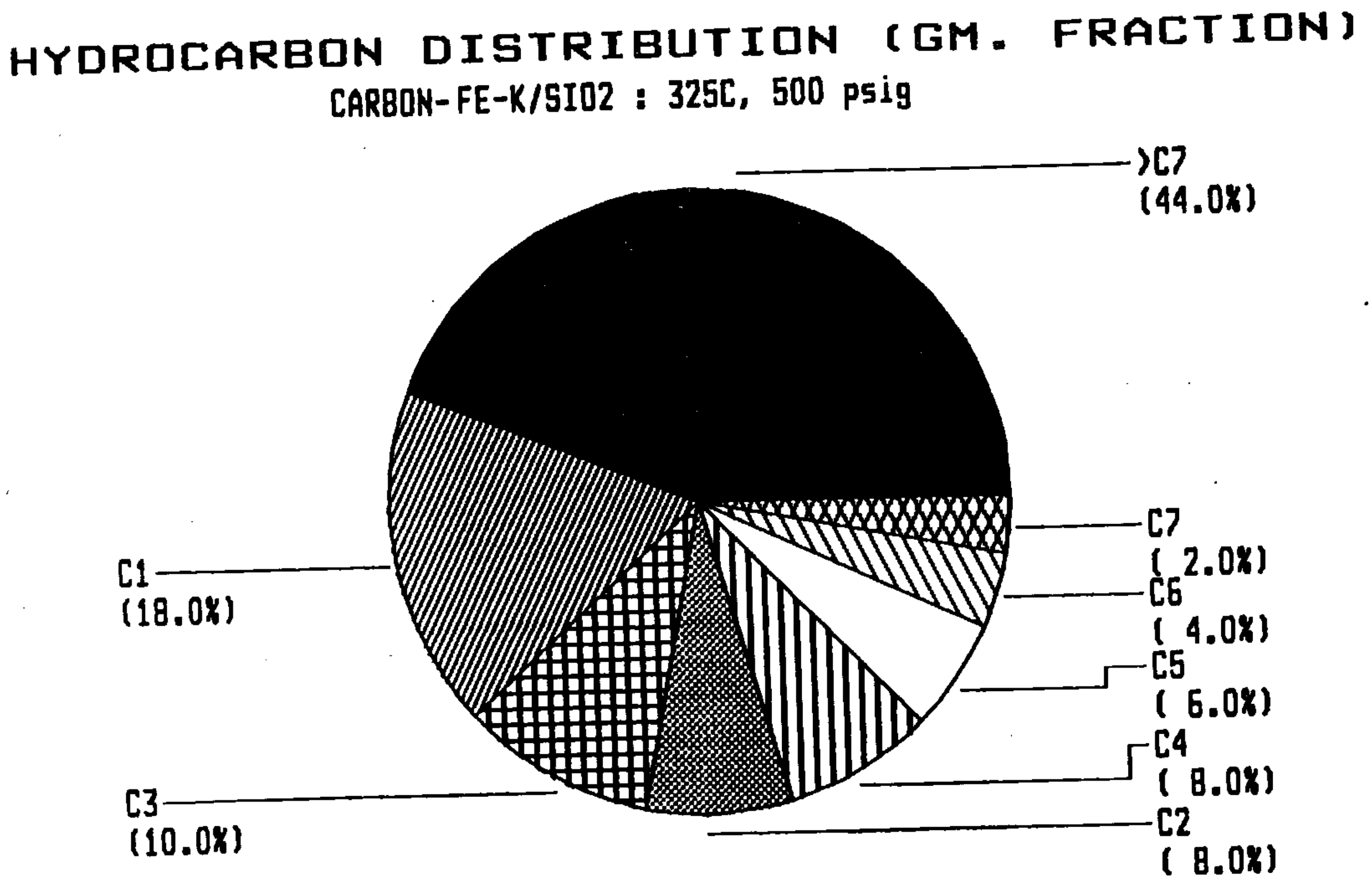

Figure 15 (b)

Gram Fractions of Products for Carbonized Fe-K/SiO_2

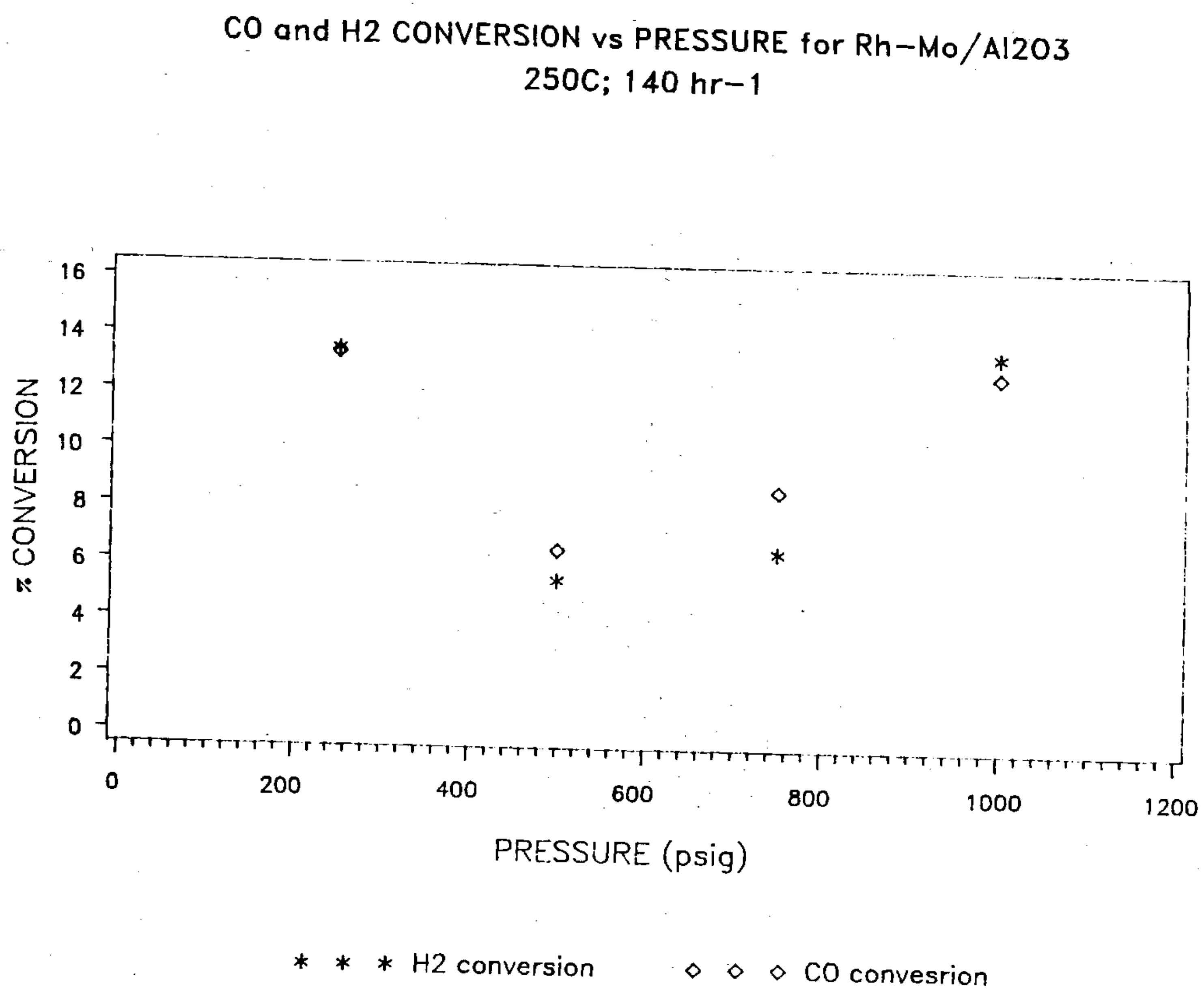

Figure 16

CO and H2 Conversions over Rh-Mo/Al_2O_3

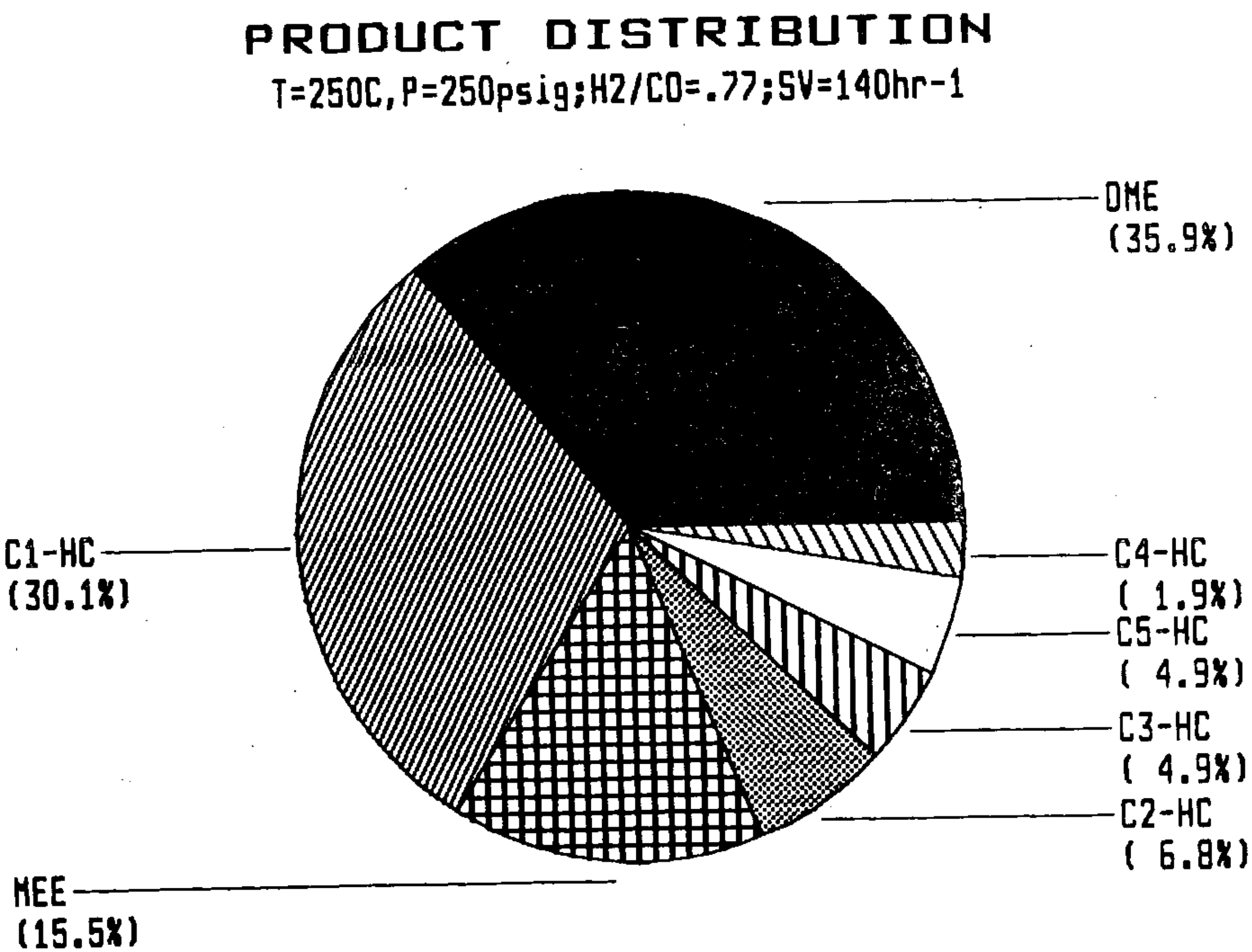

Figure 17 (a)

Product Distributions for Rh-Mo/Al_2O_3 at 250 and 970 psig

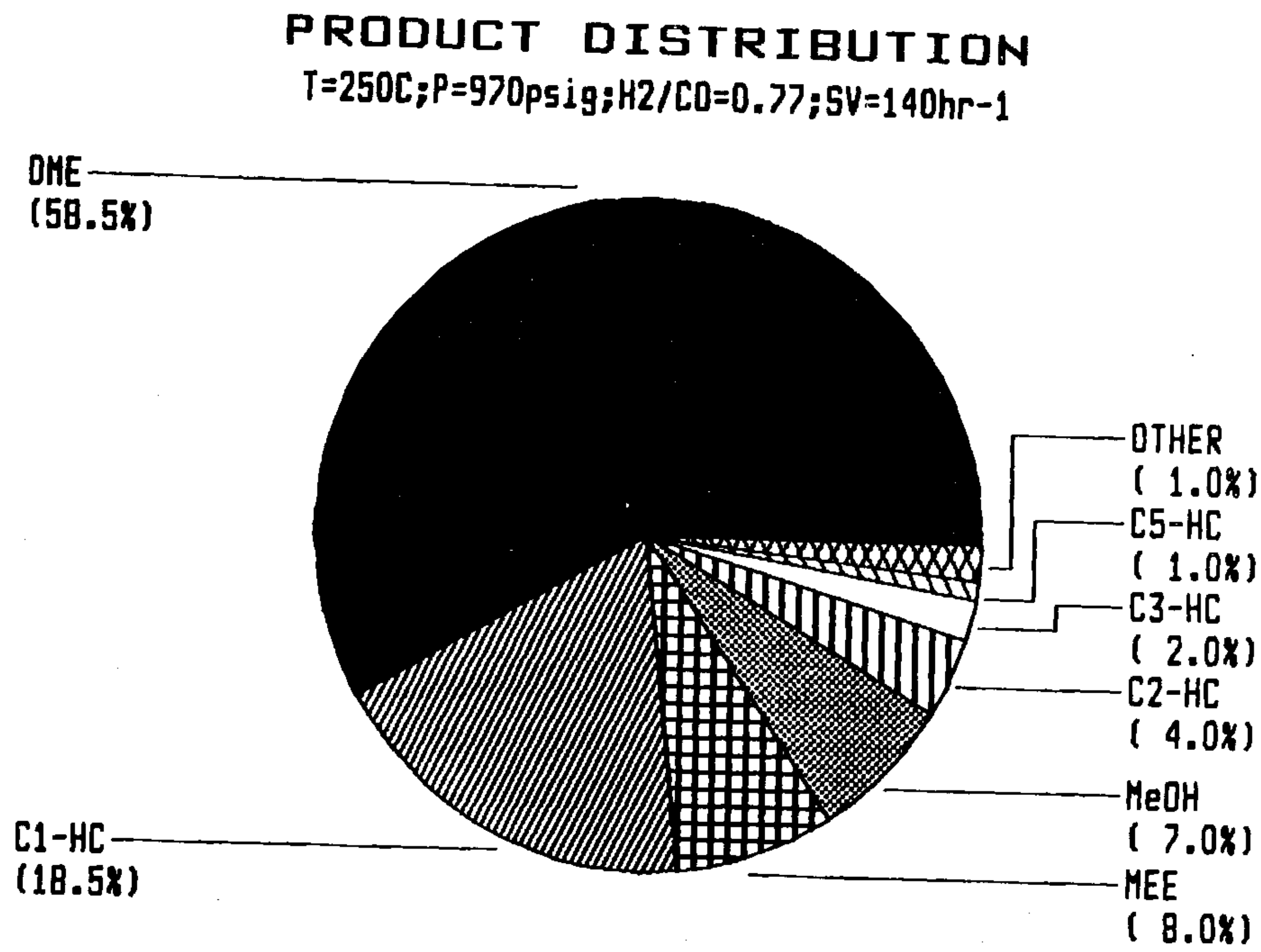

Figure 17 (b)
Product Distributions for Rh-Mo/Al_2O_3 at 250 and 970 psig

FIGURE 18

DME Yld. (g)/CH4 Yld (g) vs P (psig) for Rh–Mo/Al2O3

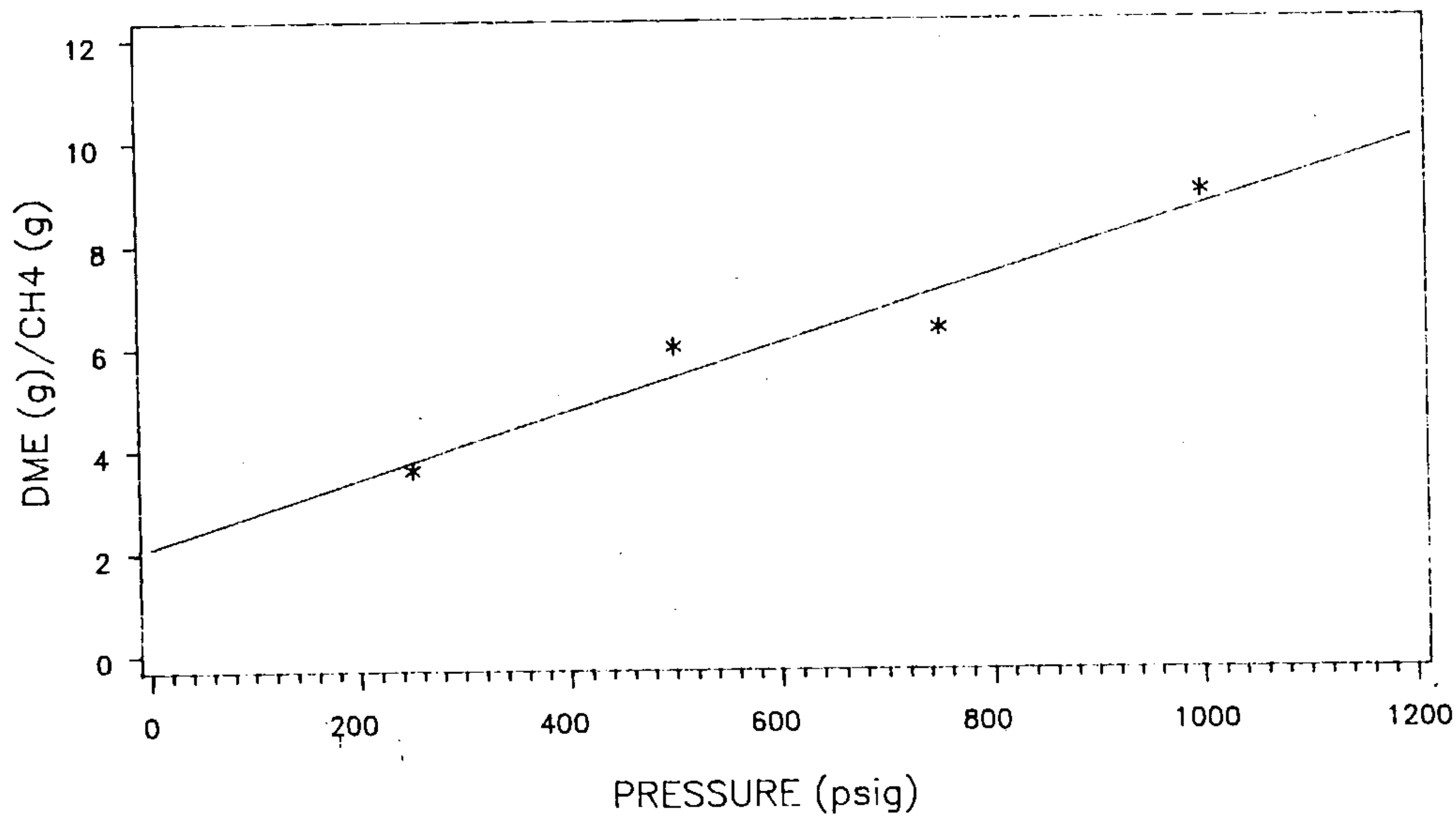

Figure 18

DME Yield/Methane Yield versus Pressure for Rh-Mo/Al_2O_3

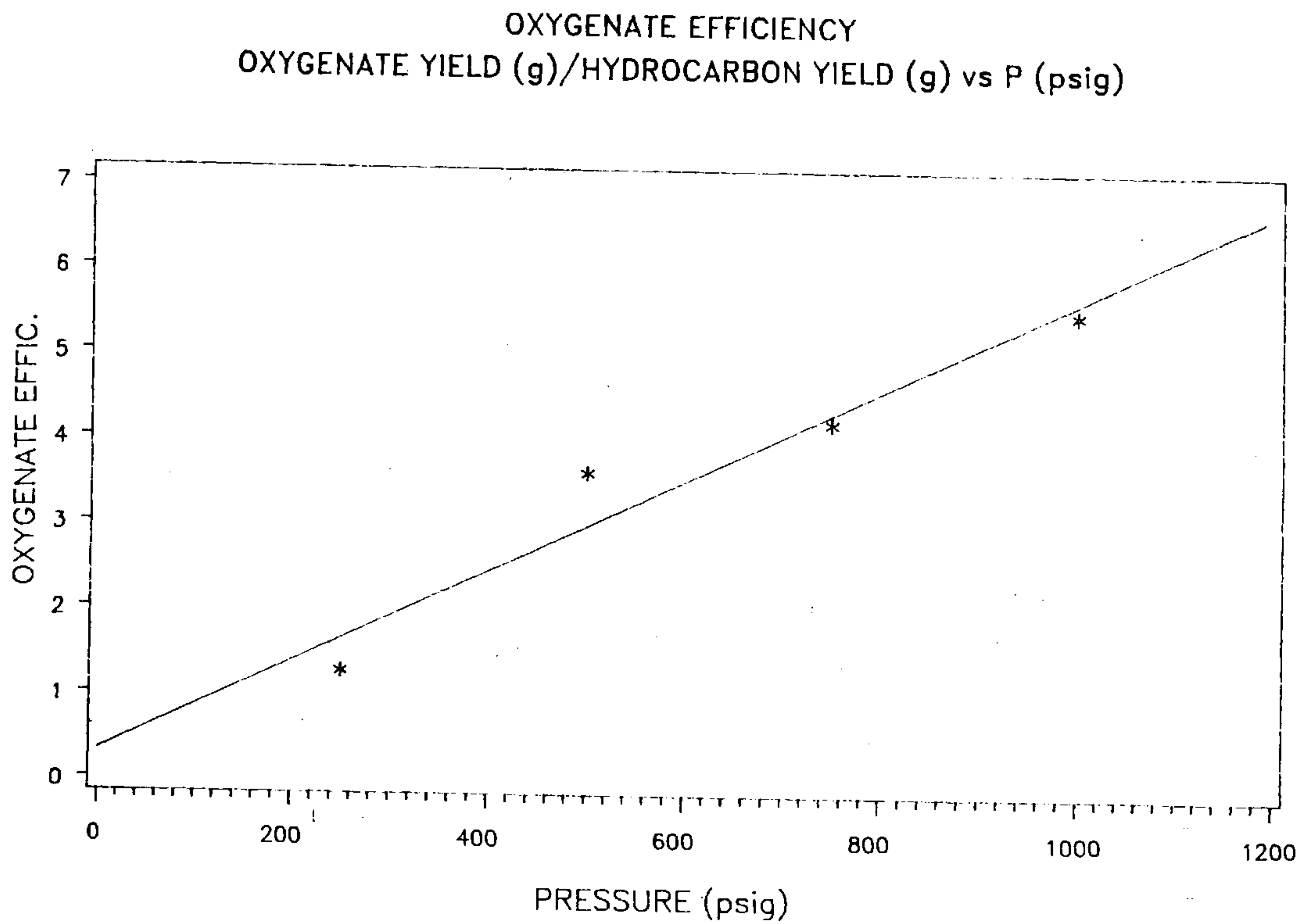

Figure 19

Overall Oxygenat Efficiency versus Pressure for $Rh\text{-}Mo/Al_2O_3$

Figure 20 (a)

CO Conversion for FT-Based Systems

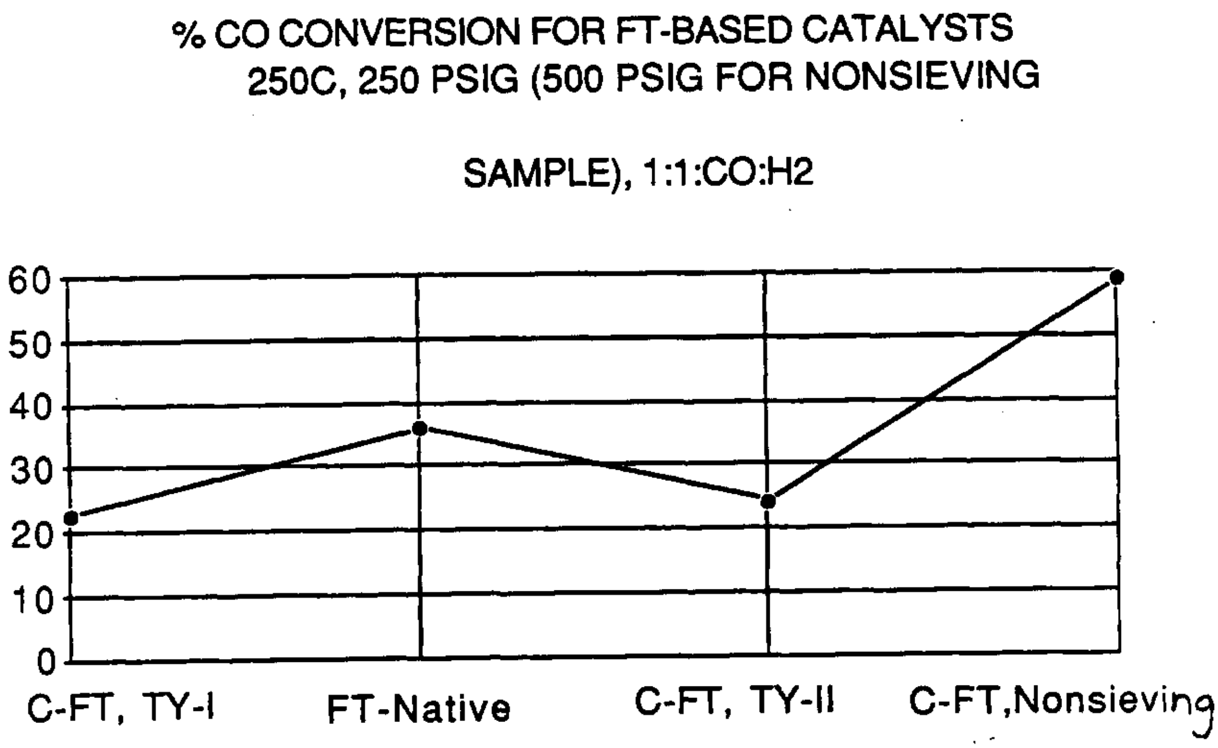

Figure 20 (b)
CO Conversion for FT-Based Systems

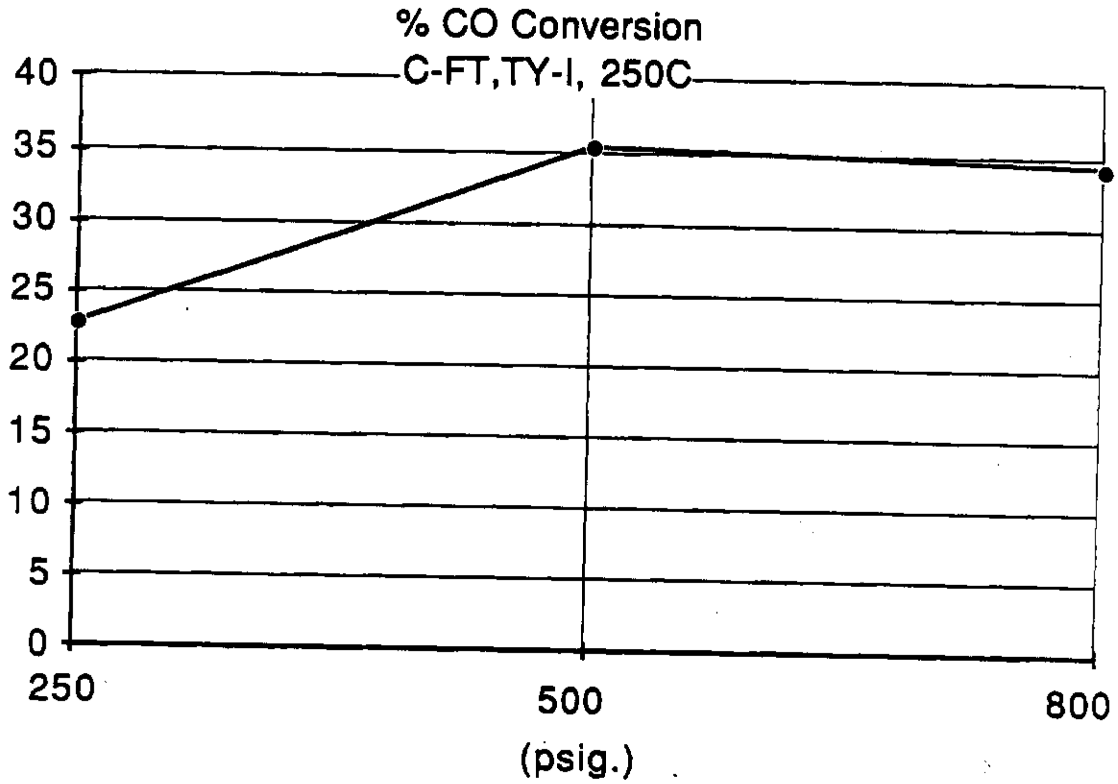

Figure 20 (c)

CO Conversion for FT-Based Systems

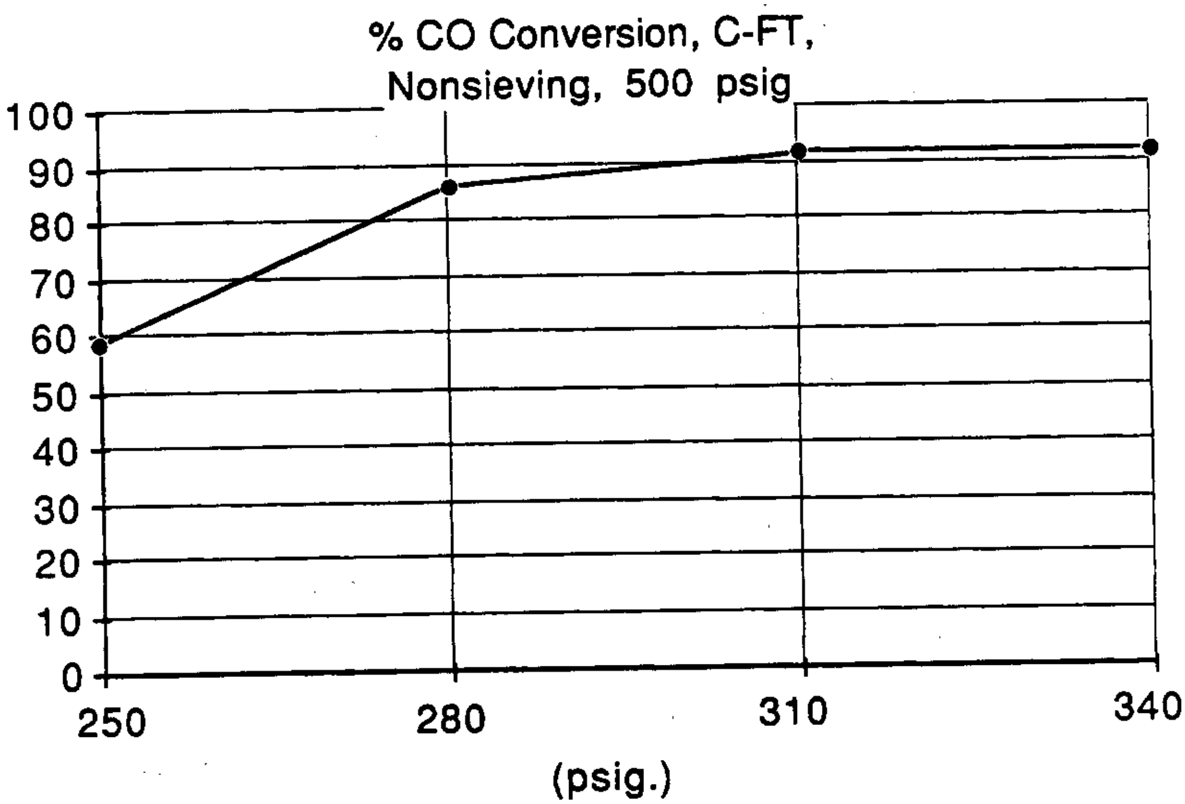

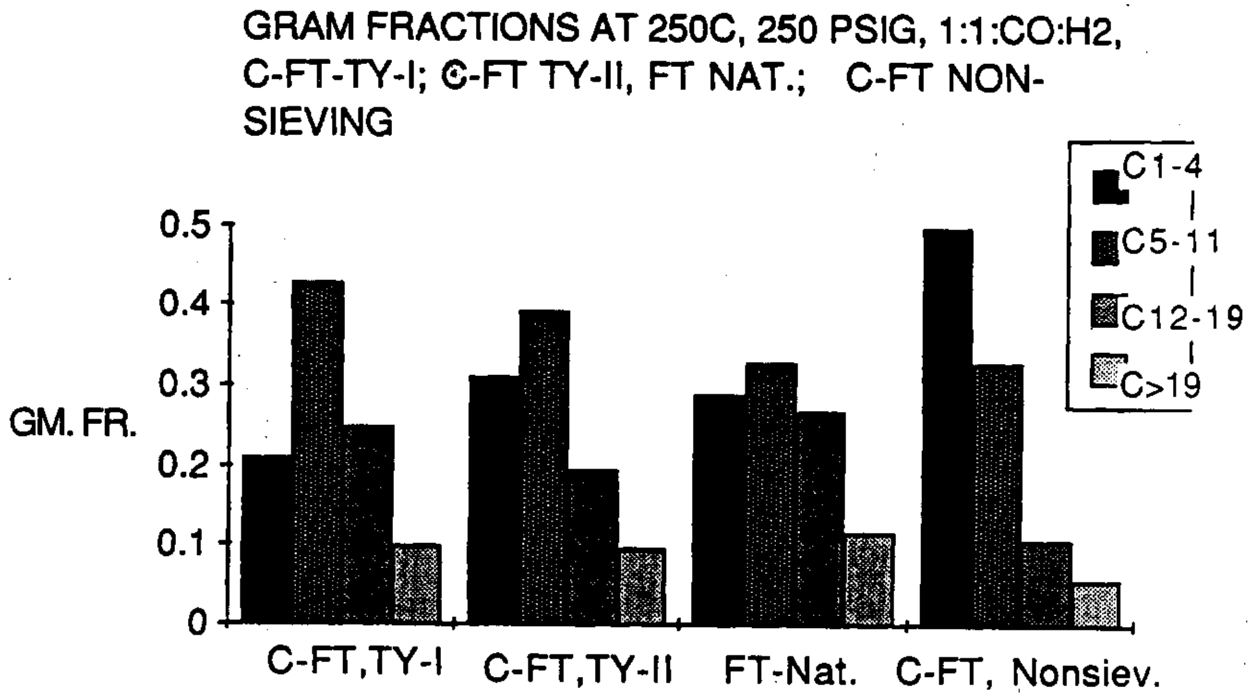

Figure 21 (a)

Gram Fractions of Products for FT-Based Materials

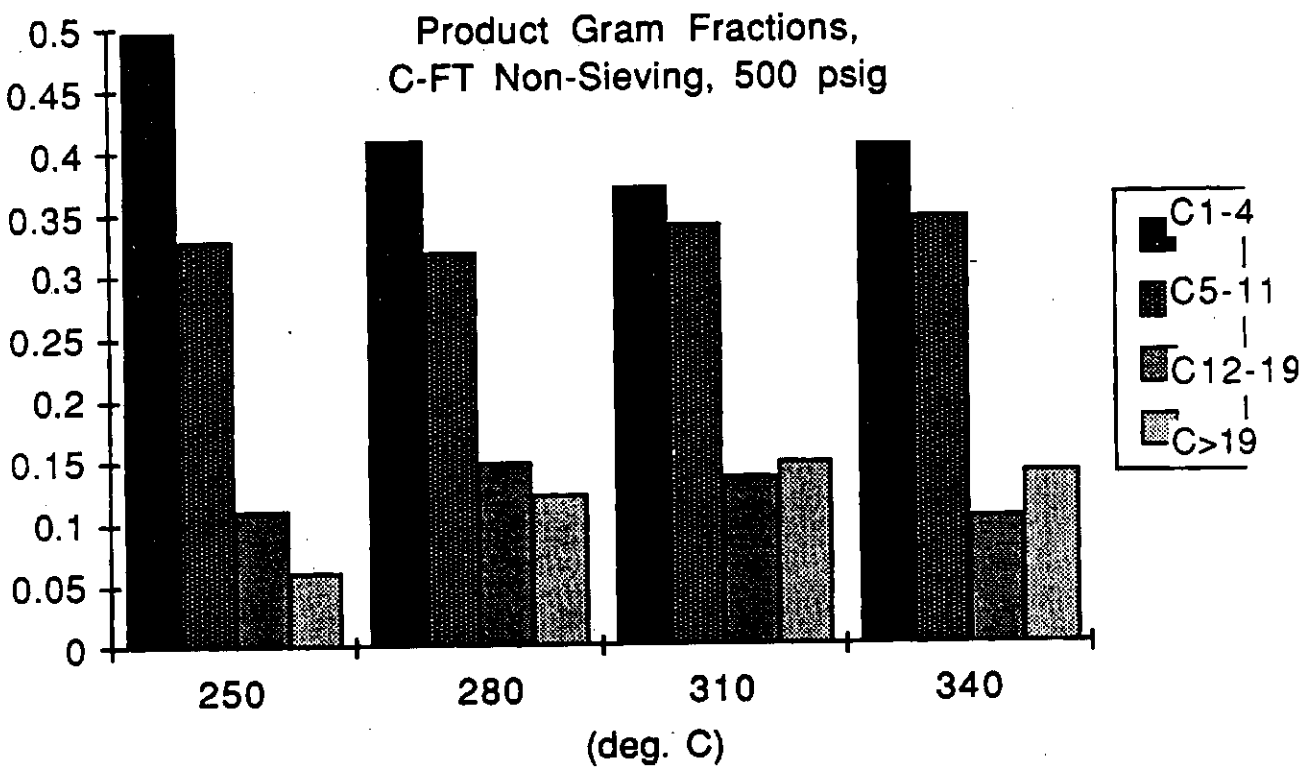

Figure 2i (b)
Gram Fractions of Products for FT-Based Materials

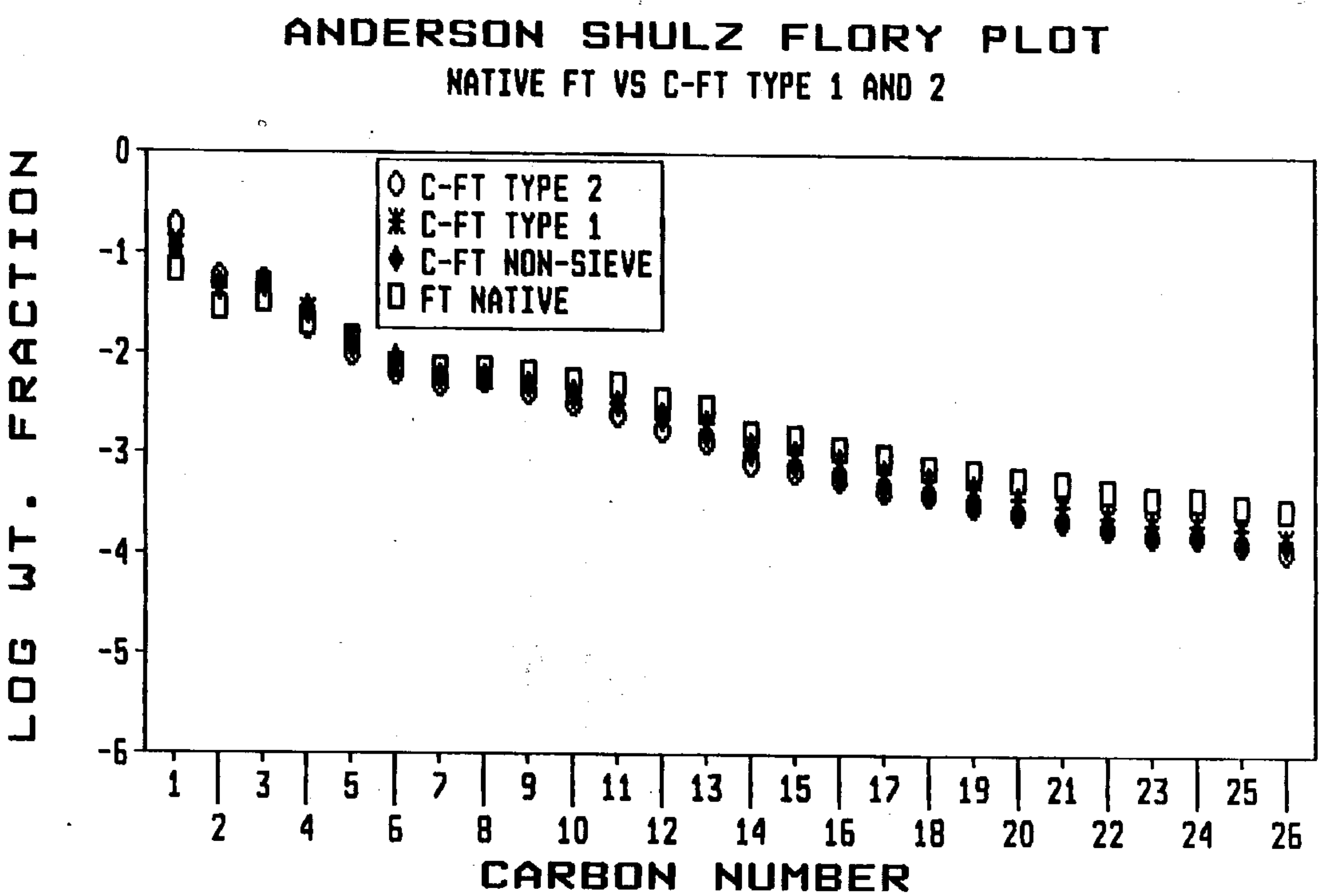

Figure 22(a)

ASF Plot for FT-Based Systems

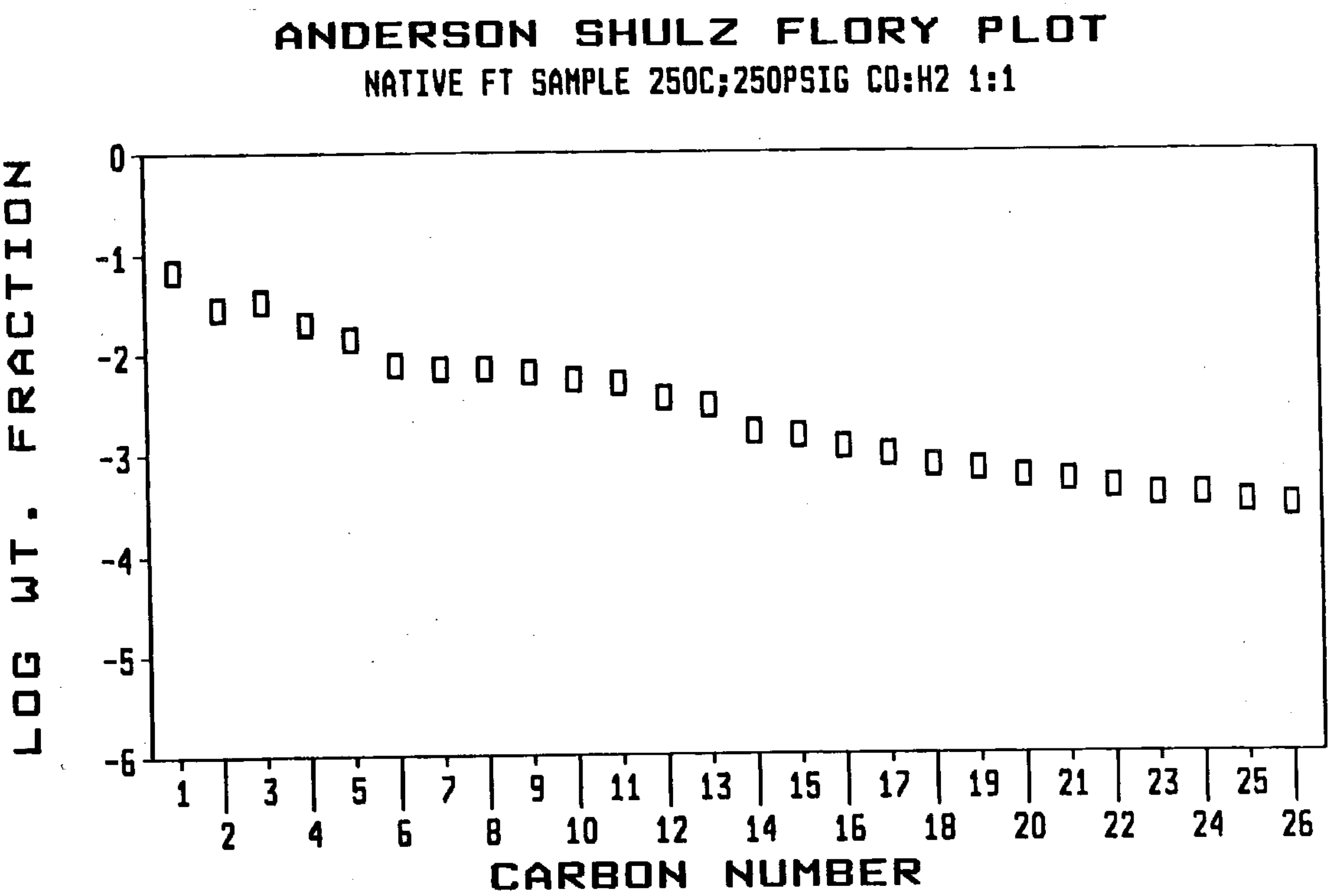

Figure 22 (b)
ASF Plot for FT-Based Systems

Figure 23

Schematic of FT-HC Concept

TYPE I - Product Selectivity
FT - Fischer Tropsch
HC - Hydrocracking

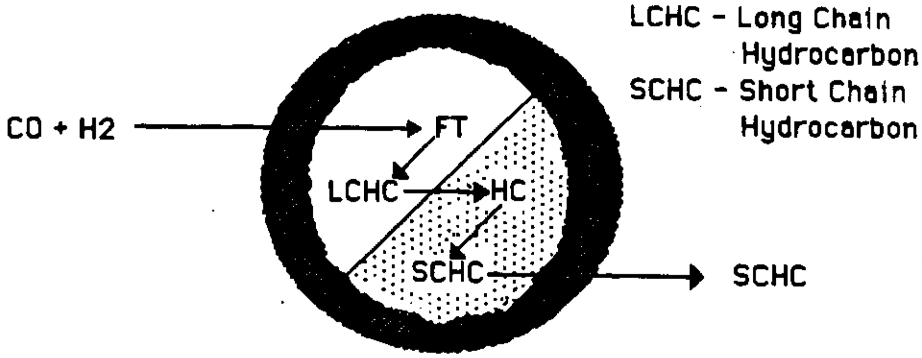

TYPE II - Transition State Selectivity

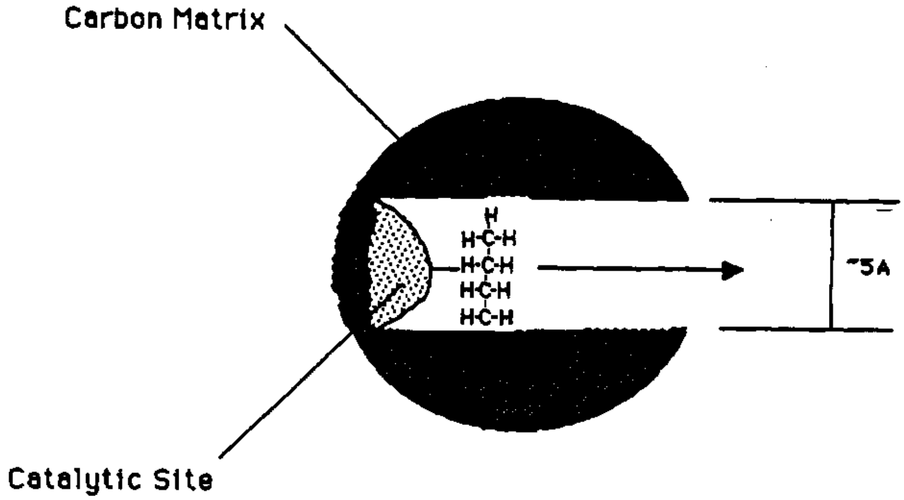

Figure 24

CO Conversion for C-FT-HC(1:1),Ty-I

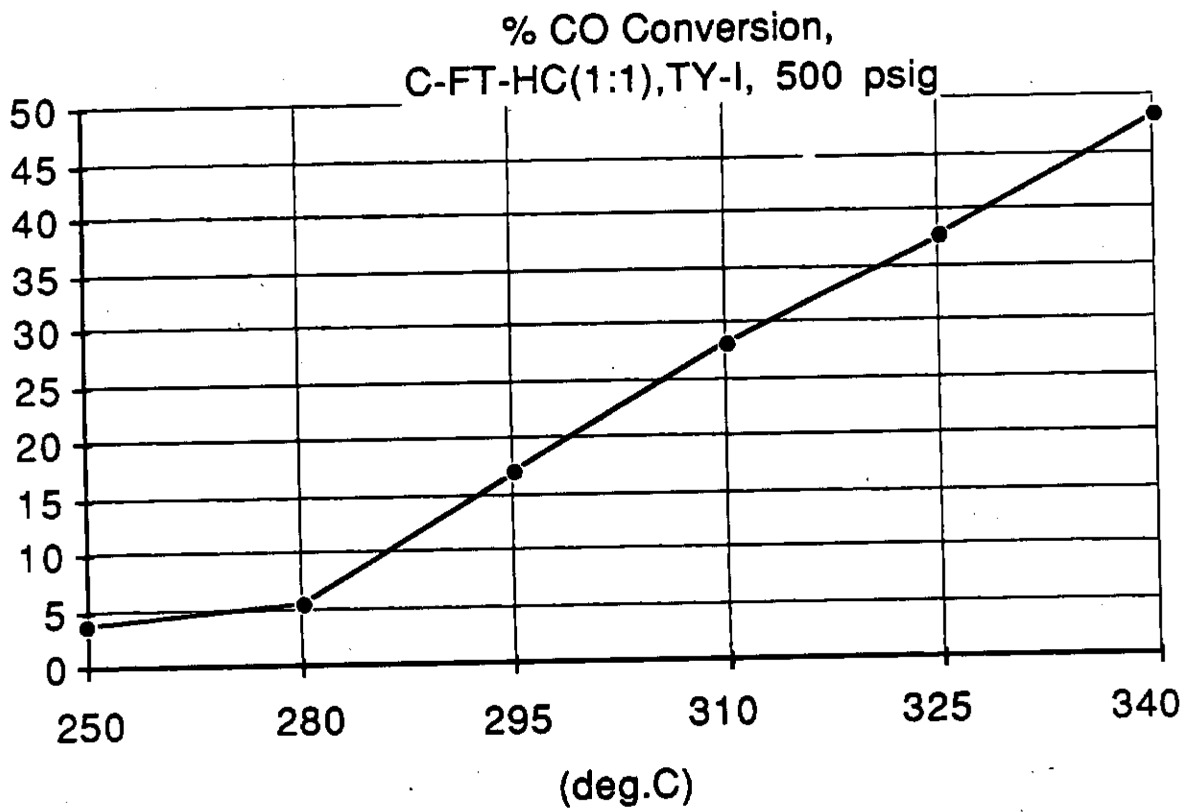

Figure 25
Gram Fractions of Products from C-FT-HC(1:1), Ty-I

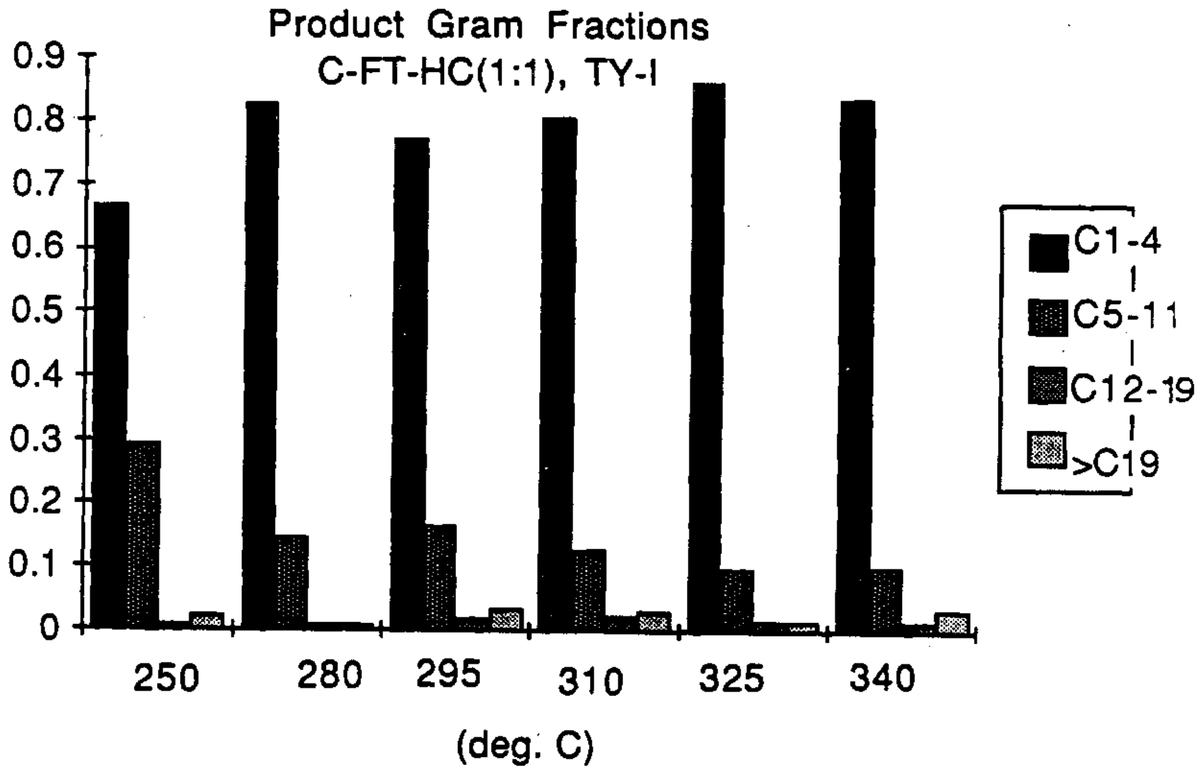

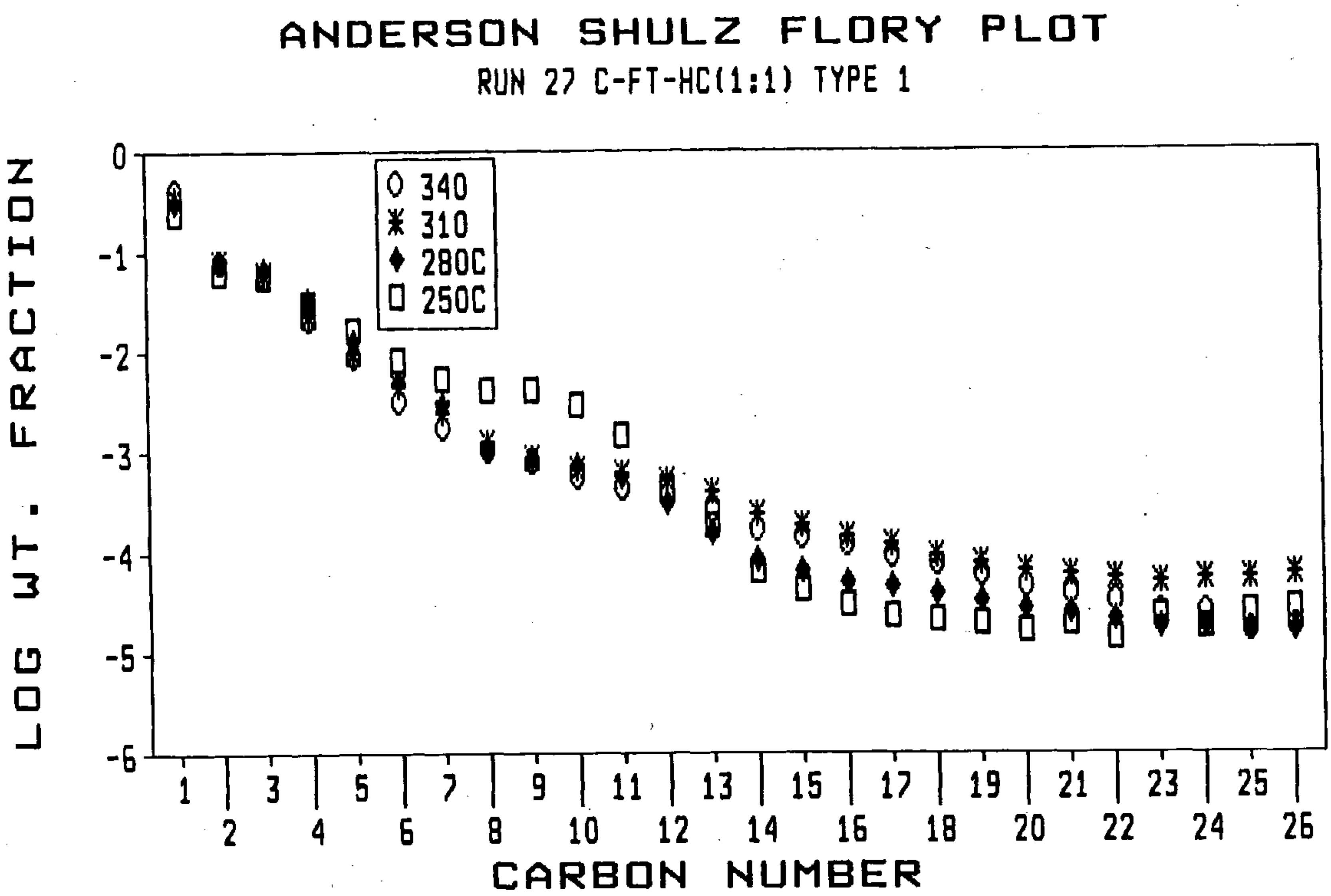

Figure 26

ASF Plots for C-FT-HC(1:1),Ty-I

Figure 27

CO Conversion for C-FT-HC(1:1),Non-Sieving

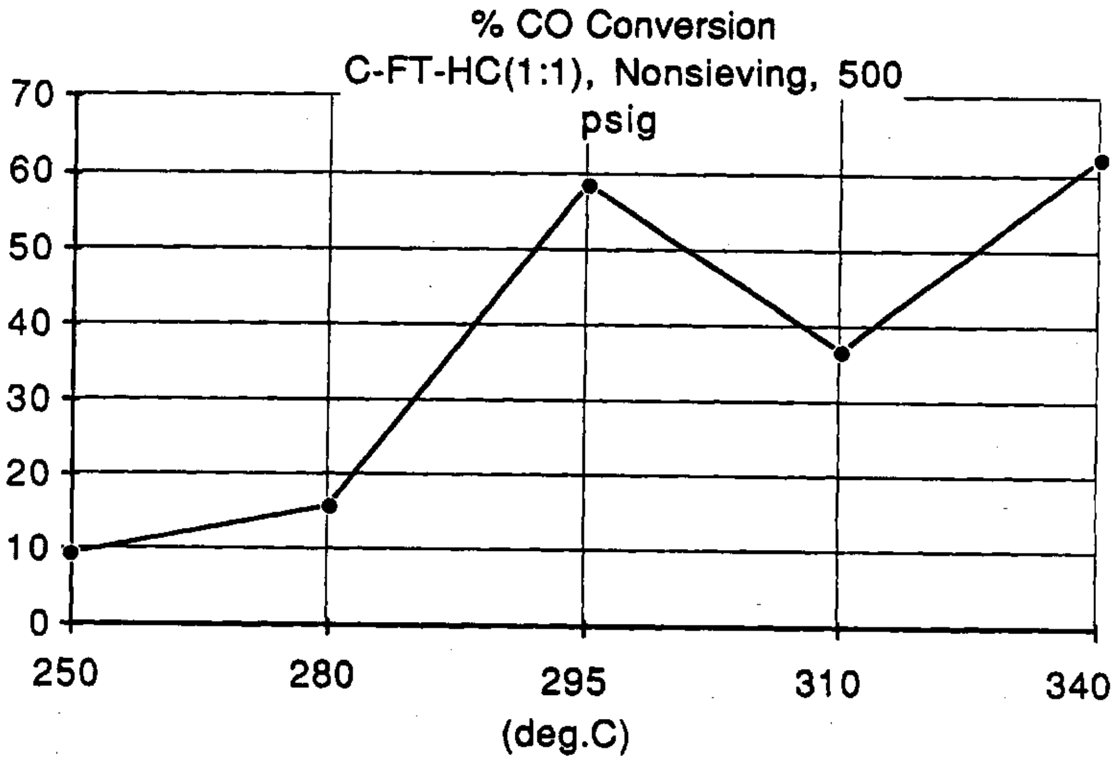

Figure 28

CO Conversion for FT-HC,Native

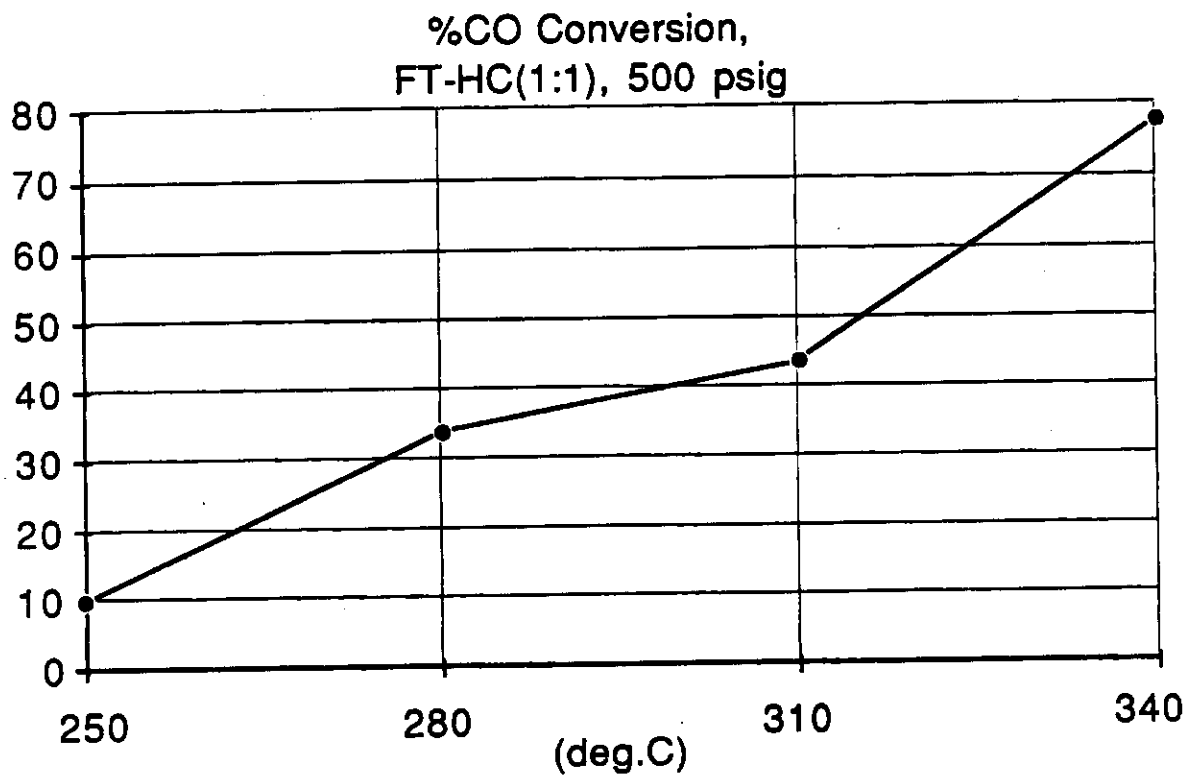

Figure 29

Gram Fractions for C-FT-HC(1:1),Non-Sieving

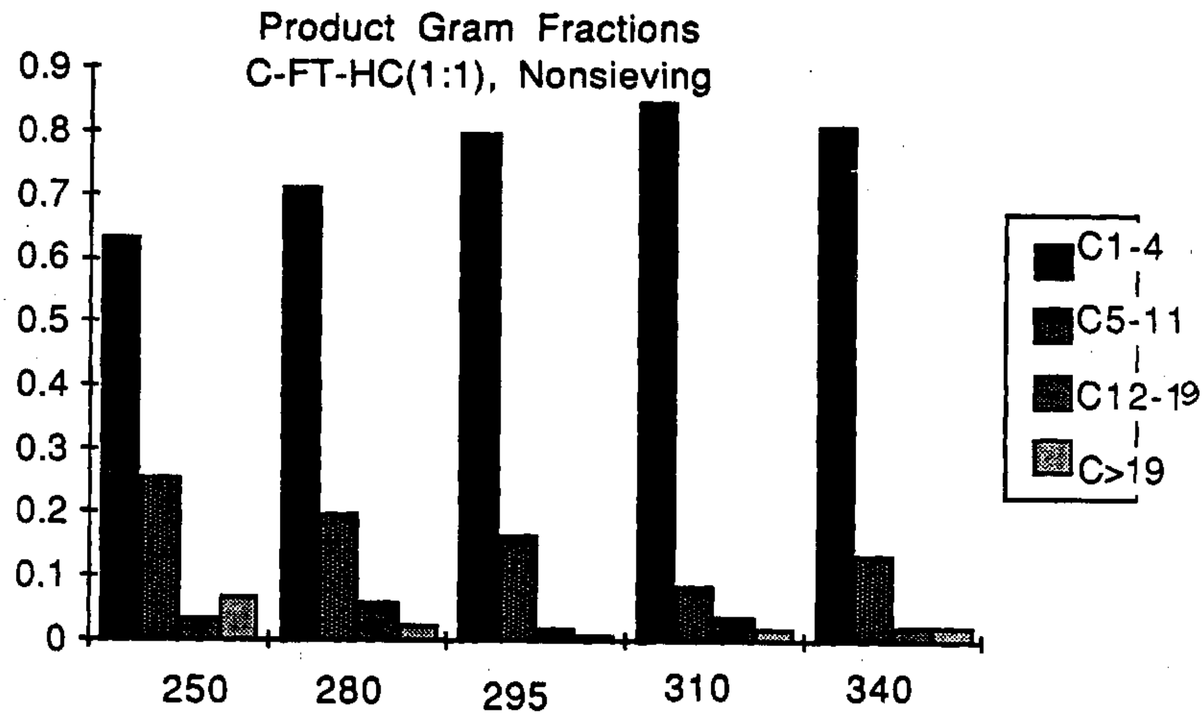

Figure 30

Gram Fractions for FT-HC,Native

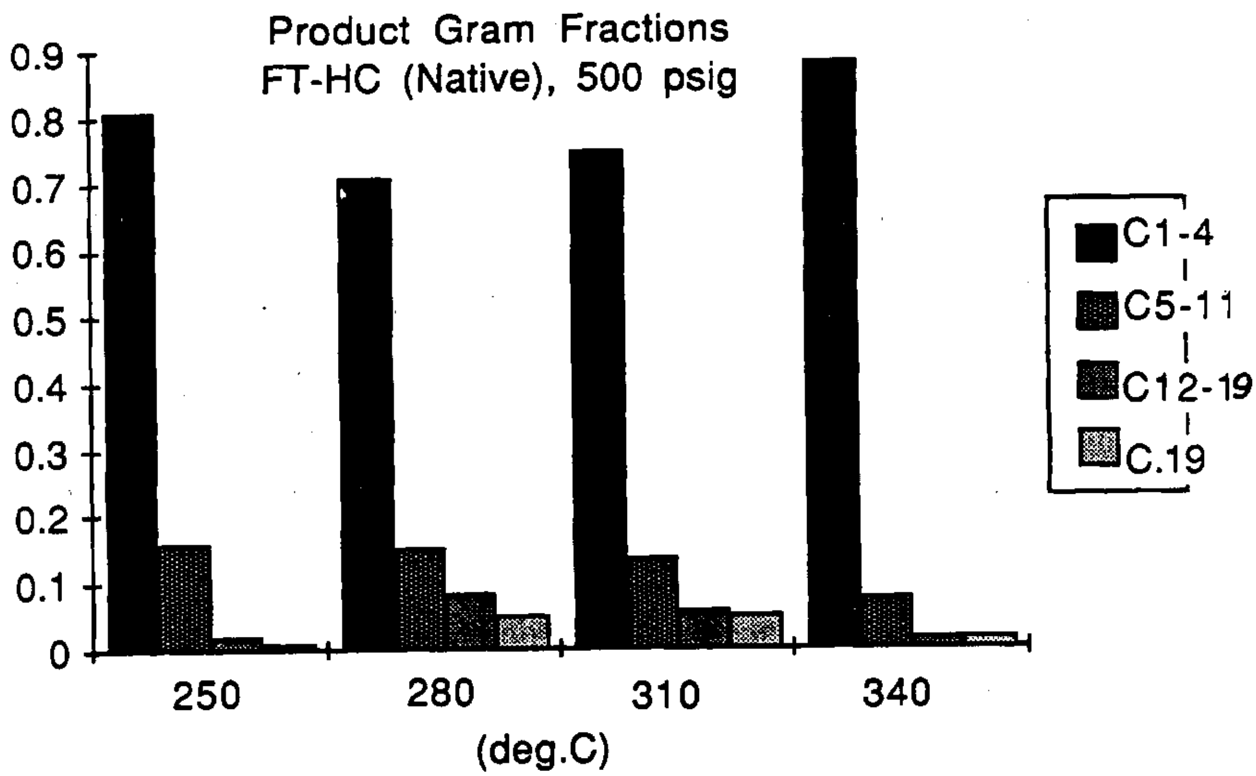

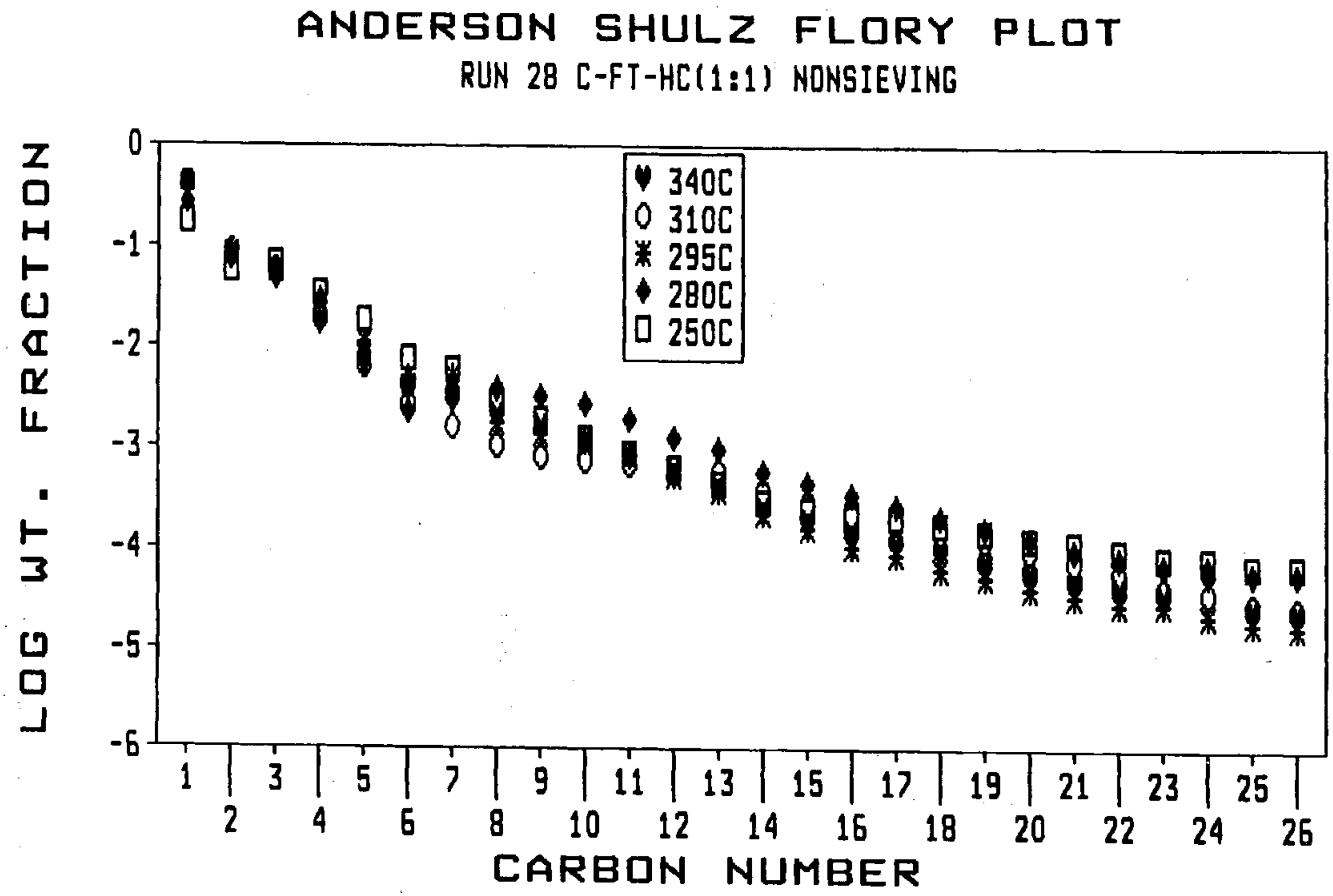

Figure 31

ASF Plots for C-FT-HC(1:1),Non-Sieving

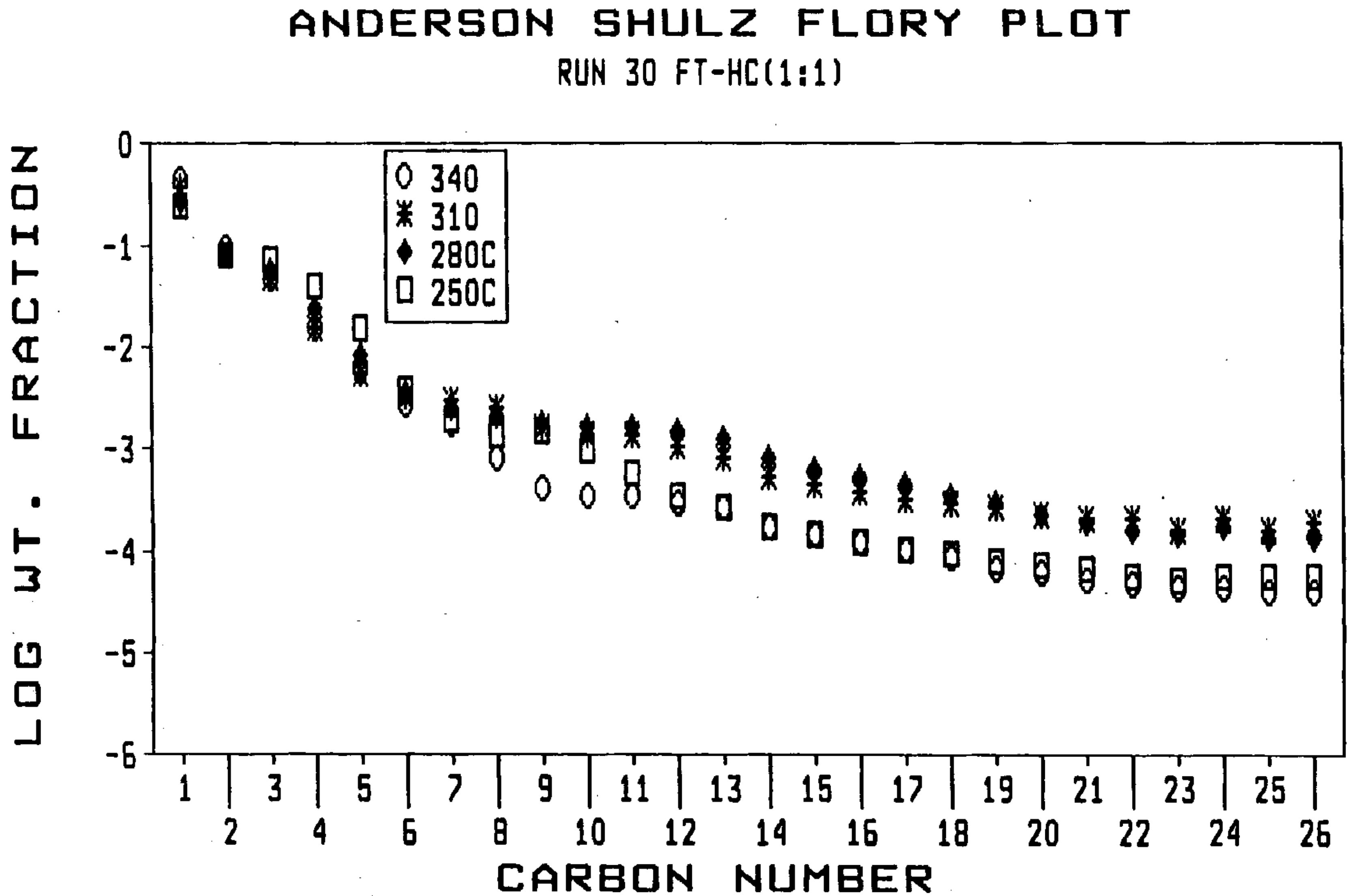

Figure 32

ASF Plots for FT-HC, Native

Figure 33

CO Conversion for C-FT-HC,Ty-I(6:1)

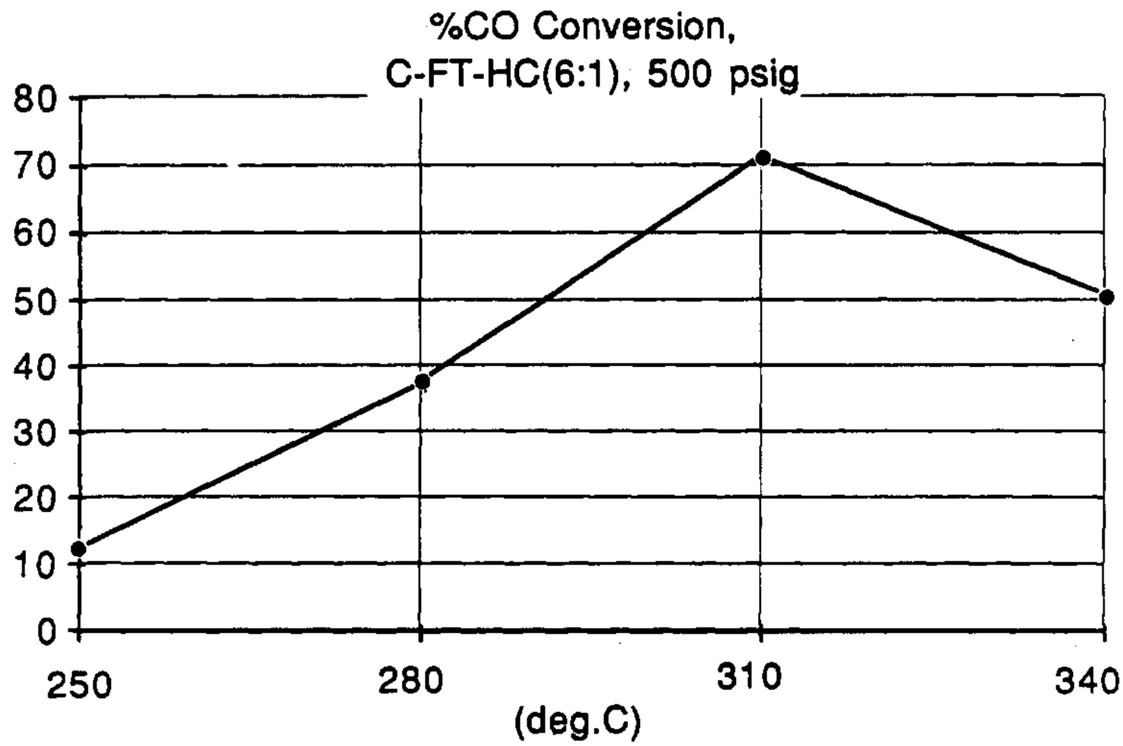

Figure 34

Gram Fractions for C-FT-HC,Ty-I(6:1)

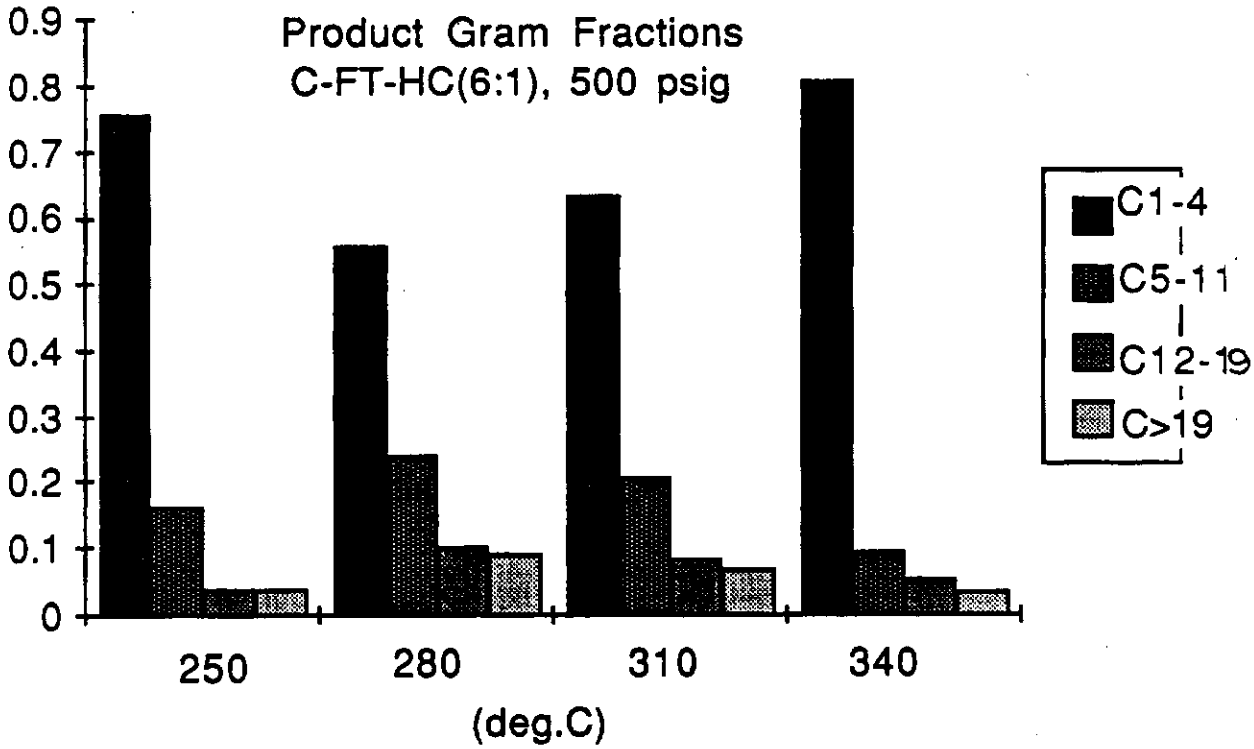

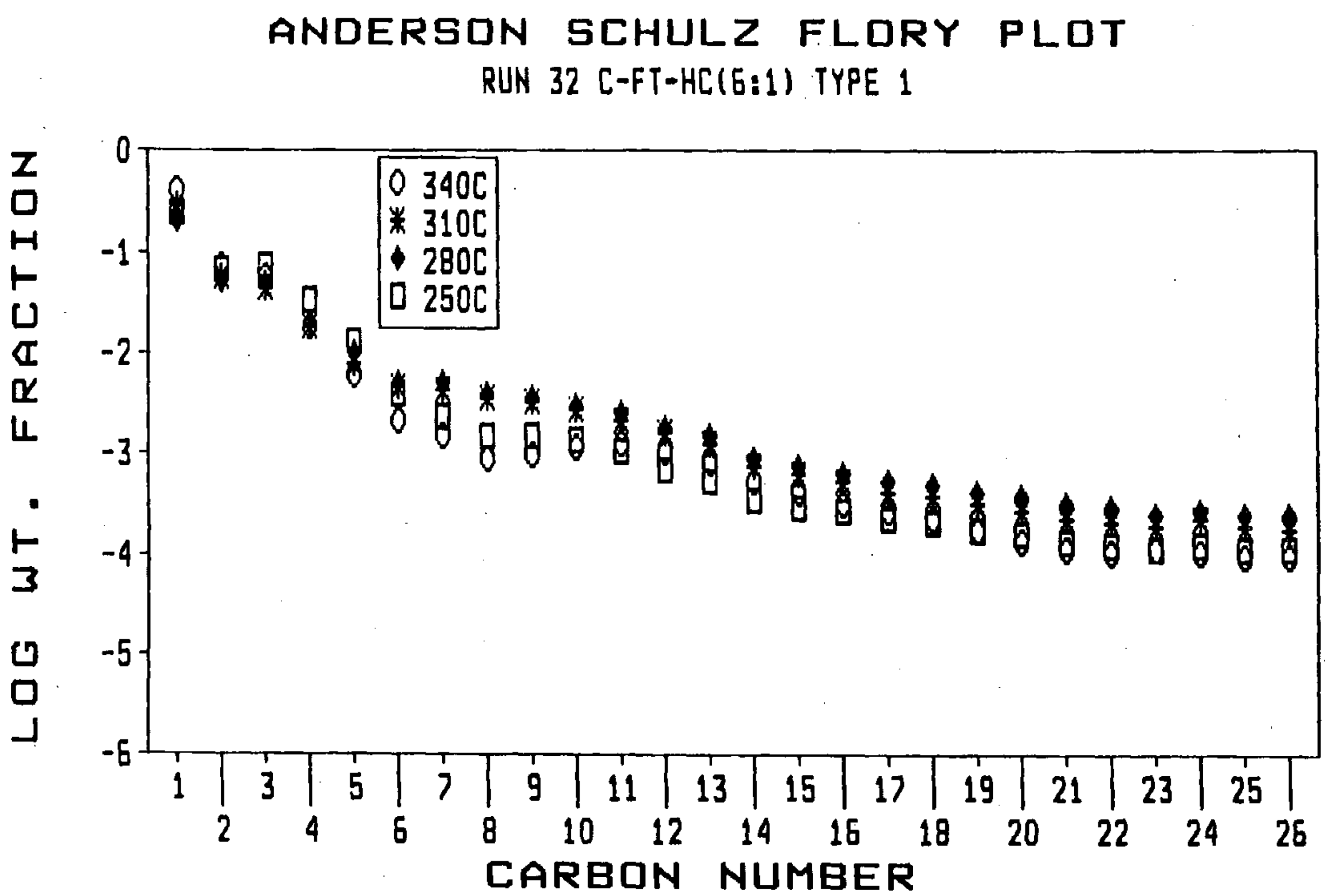

Figure 35

ASF Plots for C-FT-HC,Ty-I(6:1)

Figure 36

CO Conversion for C-FT-HC,Ty-I(3:1)

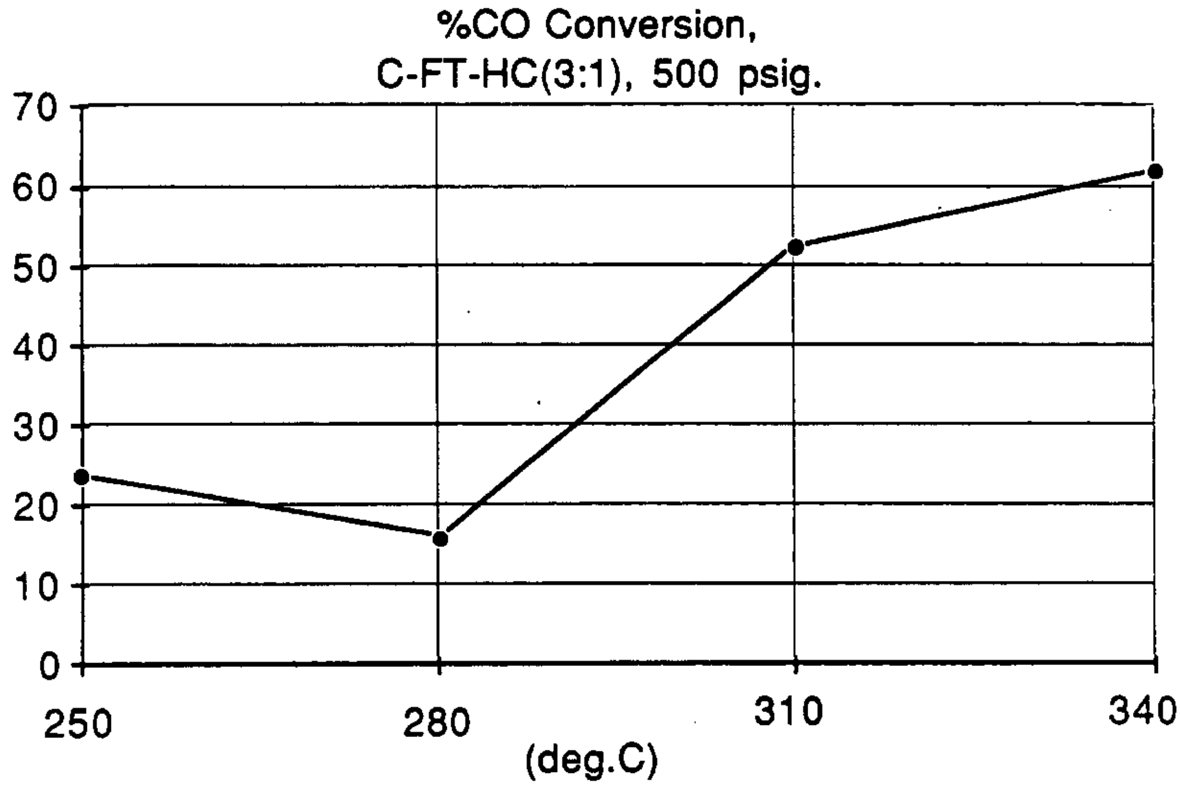

Figure 37

Gram Fractions for C-FT-HC,Ty-I(3:1)

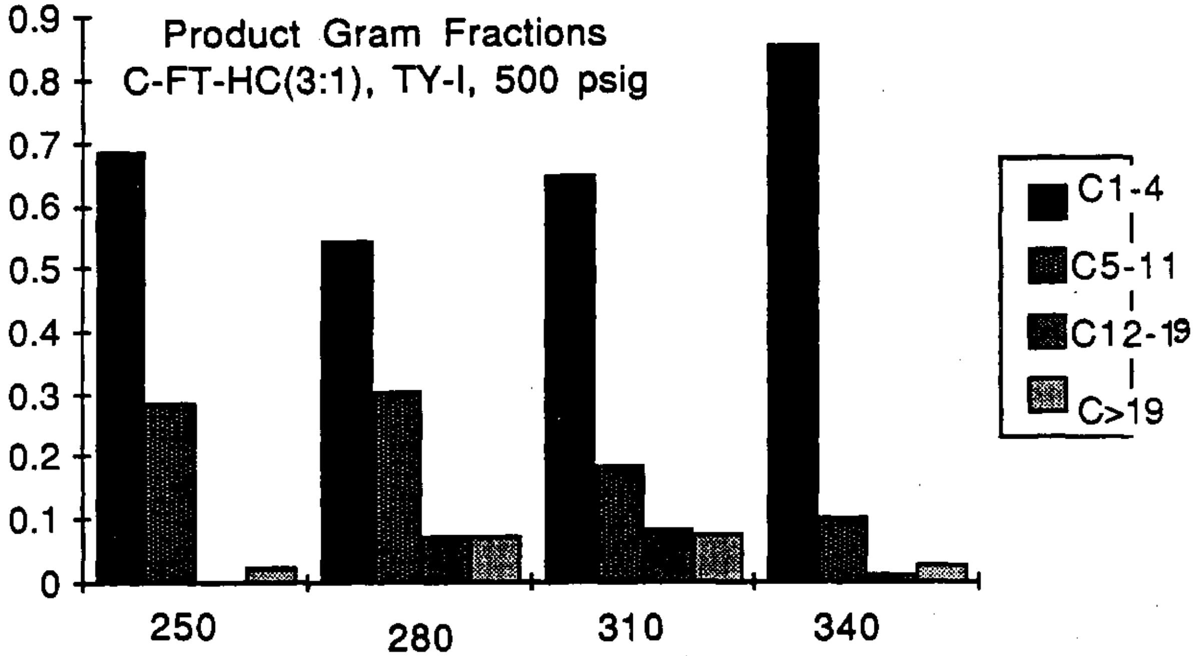

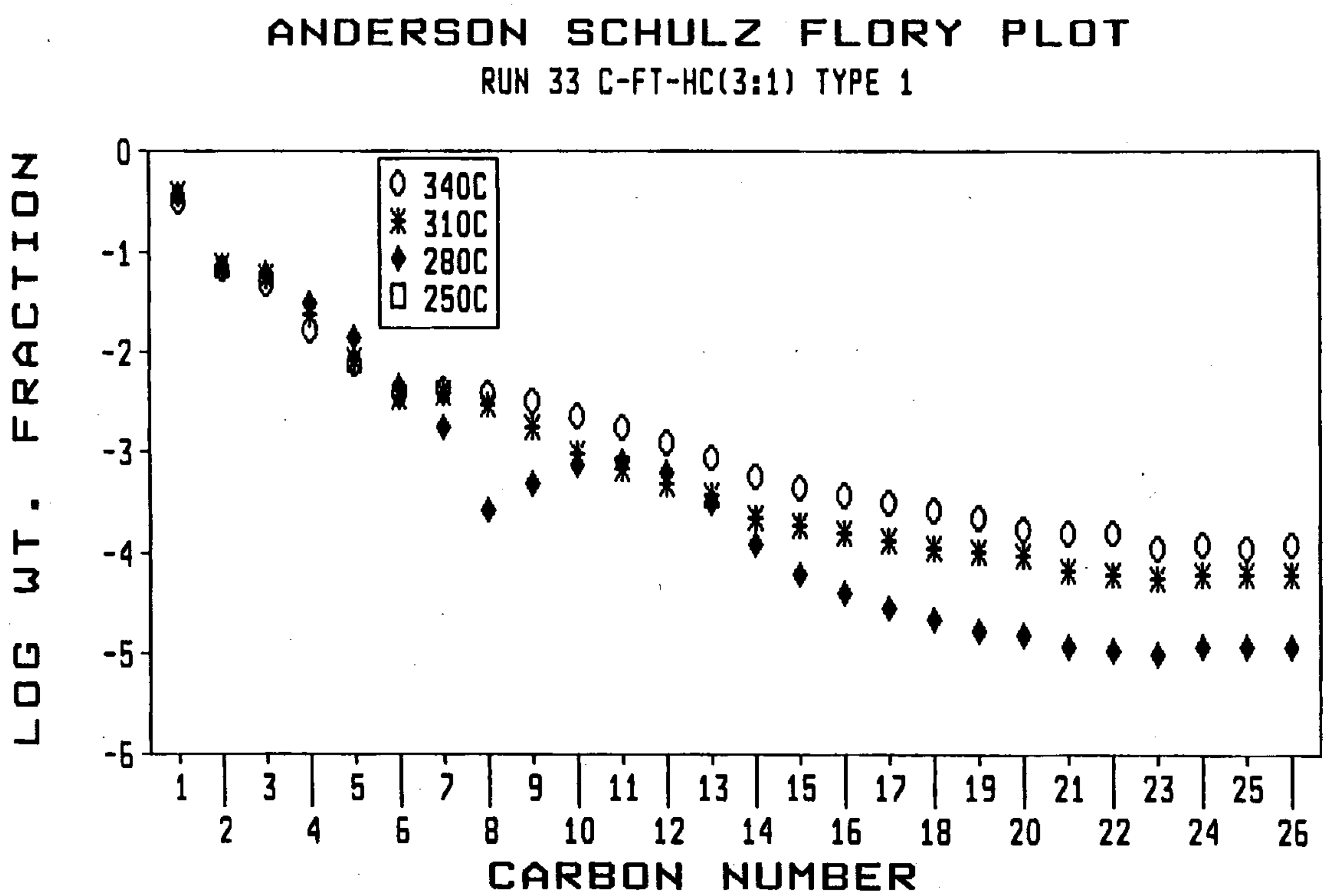

Figure 38

ASF Plots for C-FT-HC,Ty-I(3:1)

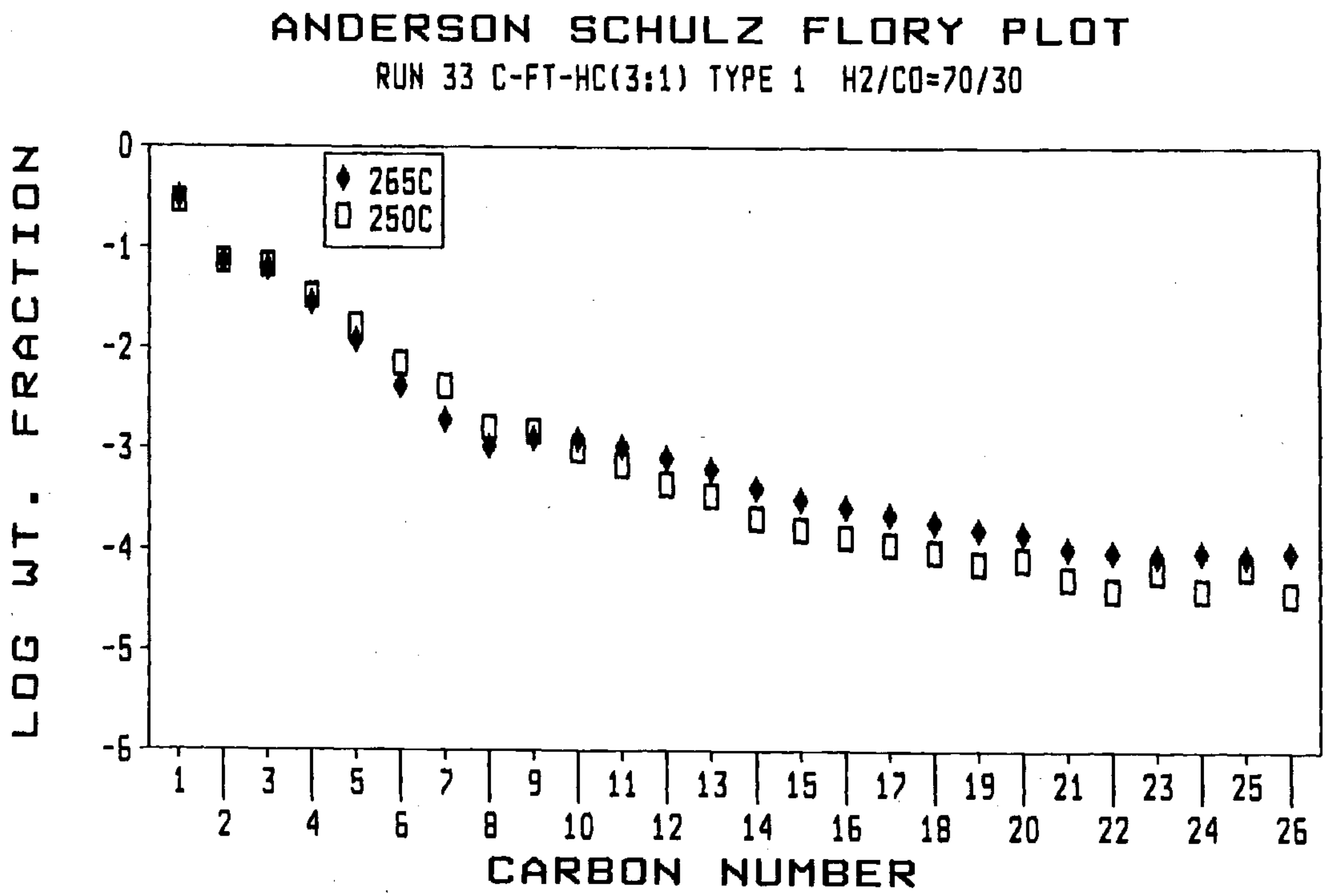

Figure 39

ASF Plots for C-FT-HC,Ty-I(3:1) with Hydrogen-Rich Feedstock